Technical University of Denmark

DTU

Combined oxidation and absorption of nox by an ionic liquid tandem process.

Fehrmann, Rasmus; Riisager, Anders; Mossin, Susanne; Jakobsen, Peter Westergaard; Madsen, Anders Theilgaard; Kunov-Kruse, Andreas Jonas

Link back to DTU Orbit

DTU Library
Technical Information Center of Denmark

(51) **International Patent Classification:**
B01D 53/04 (2006.01)

(21) **International Application Number:**
PCT/EP2015/058309

(22) **International Filing Date:**
16 April 2015 (16.04.2015)

(25) **Filing Language:** English

(26) **Publication Language:** English

(30) **Priority Data:**
14164843.6   16 April 2014 (16.04.2014)   EP

(71) **Applicant: DANMARKS TEKNISKE UNIVERSITET** [DK/DK]; Anker Engelunds Vej 101A, DK-2800 Kgs. Lyngby (DK).

(72) **Inventors: FEHRMANN, Rasmus**; Eckersbergsgade 23, DK-2100 Copenhagen Ø (DK). **RIISAGER, Anders**; Rønnevangshusene 138, DK-2630 Taastrup (DK). **MOSSIN, Susanne L.**; Gyldenløvesgade 14 st.tv., DK-1369 Copenhagen K (DK). **THOMASSEN, Peter**; Tværbommen 57, 2.th., DK-2820 Gentofte (DK). **MADSEN, Anders Theilgaard**; Markmandsgade 12, 3.tv., DK-2300 Copenhagen S (DK). **KUNOV-KRUSE, Andreas Jonas**; 35 Standish Street, Cambridge, Massachusetts 02138-6816 (US).

(74) **Agent: ZACCO DENMARK A/S**; Arne Jacobsens Allé 15, DK-2300 Copenhagen S (DK).

(81) **Designated States** *(unless otherwise indicated, for every kind of national protection available)*: AE, AG, AL, AM, AO, AT, AU, AZ, BA, BB, BG, BH, BN, BR, BW, BY, BZ, CA, CH, CL, CN, CO, CR, CU, CZ, DE, DK, DM, DO, DZ, EC, EE, EG, ES, FI, GB, GD, GE, GH, GM, GT, HN, HR, HU, ID, IL, IN, IR, IS, JP, KE, KG, KN, KP, KR, KZ, LA, LC, LK, LR, LS, LU, LY, MA, MD, ME, MG, MK, MN, MW, MX, MY, MZ, NA, NG, NI, NO, NZ, OM, PA, PE, PG, PH, PL, PT, QA, RO, RS, RU, RW, SA, SC, SD, SE, SG, SK, SL, SM, ST, SV, SY, TH, TJ, TM, TN, TR, TT, TZ, UA, UG, US, UZ, VC, VN, ZA, ZM, ZW.

(84) **Designated States** *(unless otherwise indicated, for every kind of regional protection available)*: ARIPO (BW, GH, GM, KE, LR, LS, MW, MZ, NA, RW, SD, SL, ST, SZ, TZ, UG, ZM, ZW), Eurasian (AM, AZ, BY, KG, KZ, RU, TJ, TM), European (AL, AT, BE, BG, CH, CY, CZ, DE, DK, EE, ES, FI, FR, GB, GR, HR, HU, IE, IS, IT, LT, LU, LV, MC, MK, MT, NL, NO, PL, PT, RO, RS, SE, SI, SK, SM, TR), OAPI (BF, BJ, CF, CG, CI, CM, GA, GN, GQ, GW, KM, ML, MR, NE, SN, TD, TG).

Published:

— *with international search report (Art. 21(3))*

(54) **Title:** COMBINED OXIDATION AND ABSORPTION OF NOx BY AN IONIC LIQUID TANDEM PROCESS

(57) **Abstract:** The present invention relates to a new strategy for capturing NOx using a two-step process.
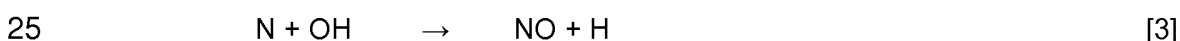
Combined oxidation and absorption of NO_x by an ionic liquid tandem process

The present invention concerns a new strategy for capturing NO_x using a two-step process.

5   **Background**

NO_x is a generic term for the various nitrogen oxides produced during combustion or NO_x being present in off-gasses in general. Nitrogen oxides are believed to aggravate asthmatic conditions, react with the oxygen in the air to produce ozone, which is also an irritant, and eventually form nitric acid when dissolved in water. In atmospheric

10   chemistry the term NO_x means the total concentration of NO, NO_2, N_2O, N_2O_3, N_2O_4 and N_2O_5. The man made emission of NO_x is of environmental concern since NO_x participates in detrimental photochemical reactions in both the troposphere and the stratosphere. NO_x reacts with hydrocarbon containing pollutants forming health-threatening smog in densely populated areas as well as being active in depleting the

15   ozone layer. The end product, NO_2, contributes to acid rain which can damage both trees and entire forest ecosystems. Consequently, the sources of NO_x emissions are now being subjected to more stringent standards.

Nitrogen oxides can be formed during the combustion of nitrogen precursors in the

20   fuel, defined as fuel NO_x, but also from the nitrogen in the air via two mechanisms, one designated as thermal NO_x, via the Zeldovich mechanism:

$$O + N_2 \quad\rightarrow\quad NO + N \quad\quad\quad\quad\quad\quad\quad\quad [1]$$

$$N + O_2 \quad\rightarrow\quad NO + O \quad\quad\quad\quad\quad\quad\quad\quad [2]$$

25
$$N + OH \quad\rightarrow\quad NO + H \quad\quad\quad\quad\quad\quad\quad\quad [3]$$

The other is designated as prompt NO_x, where the nitrogen in air is fixed by hydrocarbon radicals and subsequently oxidized to NO_x [G. Löffler et al. *Fuel*, vol. 85, pp. 513–523, 2006]:

30

$$N_2 + CH \quad\rightarrow\quad HCN + N \quad\quad\quad\quad\quad\quad\quad\quad [4]$$
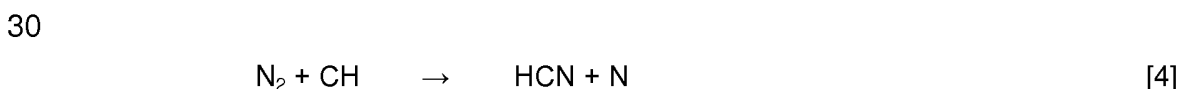
Three primary sources of NO_x formation in combustion processes are documented, the three processes being thermal NO_x (reactions [1]-[3]), fuel NO_x and prompt NO_x

35   (reaction [4]).

Thermal NO_x formation, which is highly temperature dependent, is recognized as the most relevant source when combusting e.g. natural gas. Due to the high energy required to break the nitrogen triple bond – i.e. reaction scheme [1] – thermal NO_x is
5   primarily produced at high temperatures, usually above 1200°C [H. Bosch et al. *Catal. Today*, vol. 46, pp. 233–532, 1988].

From a thermodynamic point of view, the reaction $N_2 + O_2 \rightarrow 2NO$ is thermodynamically highly unfavored with a reaction enthalpy of $\Delta H^o_{298\,K} = 180$ kJ/mol
10   [G. Busca et al. *Catal. Today*, vol. 107–108, pp. 139–148, 2005]. Therefore it requires very high temperatures to proceed at a reasonable rate. The formation of the various nitrogen compounds, N_2O, NO or NO_2, depends on the oxygen partial pressure, due to the increasing O/N ratio.

15   Another source of NO_x production from nitrogen containing fuels, such as certain coals and oil, is the conversion of chemically bound nitrogen in the fuel to NO_x during combustion. The nitrogen bound in the fuel is released exemplified by the following reaction:

20          $$4\,NH_3 + 5\,O_2 \quad \rightarrow \quad 4\,NO + 6\,H_2O \qquad\qquad\qquad\qquad [5]$$
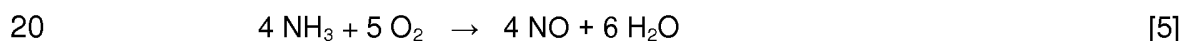
where the nitrogen containing compounds, like ammonia and amines, are oxidized to NO. The reaction is thermodynamically highly favoured, with a reaction enthalpy of $\Delta H^o_{298\,K} = -452$ kJ, although less favoured than the oxidation of NH_3 to N_2. The amount
25   of formed 'fuel NO_x' primarily depends on the amount of nitrogen in the fuel, and is also strongly influenced by the reactor design. In natural gas (methane), nitrogen compounds are virtually absent, but substantial amounts of nitrogen is present in the case of coal, gas oils and fuel oils and especially in biofuels, such as wood.

30   Prompt NO_x is generated when the fuel-to-air ratio is high and nitrogen radicals formed in reaction [4] react with oxygen via reaction [2]. The reactions are almost not temperature dependent, but the prompt NO_x formed is negligible relative to thermal NO_x.

The numerous possibilities to reduce NO_x can be divided into three categories; precombustion, combustion modifications and post combustion.

The precombustion strategy imply using alternative fuels with a lower content of nitrogen species. During combustion different types of modifications can be utilized, of which the most used are; low NO_x-burners, reburning (exhaust gas recirculation) and staged air combustion (thermal oxidation). A variety of other methods are also possible in the combustion modification; burners out-of-service, derating, burner system modification, trim and diluent injection.

Several post-combustion approaches are applied to reduce NO_x; selective catalytic reduction (SCR), selective non-catalytic reduction (SNCR), absorption, NO_x recycle, direct decomposition, photocatalytic oxidation, multifunctional filter (removal of fly-ash and NO_x) and pulse intense electron beam irradiation.

A different concept is presented by wet scrubbing systems for removal of SO_2, SO_3 and NO_x. Some aqueous scrubbing systems have been developed for the simultaneous removal of NO_x and SO_2 [C.-L. Yang et al. *Environmental Progress*, **17**, *80–85* (1998)]. The wet flue gas desulfurization (FGD) typically exhibits high SO_2 removal efficiencies, but the FGD can only remove a small amount of NO_x because about 90–95% in a typical flue gas is present as insoluble NO and only the remaining 5-10% NO_2 is water soluble.

Attempts to oxidize NO to water soluble NO_2 have been made by adding strong oxidizing additives, such as MnO_4^- salts and H_2O_2, but the treatment cost involved herein has been too high for practical utilization.

Promising results of the simultaneous NO and SO_2 removal in a $[Co(NH_3)_6]^{2+}$ solution, which operates below 80°C, have been reported by Long et al. [X.-I. Long et al., *Industrial & Engineering Chemistry Research*, **43**, *4048–4053* (2004)].

Another approach for removing NO is the complexation of NO with Fe^{2+}-chelates based on ethylenediaminetetraacetic acid (EDTA) or nitrilotriacetate (NTA), as outlined in reaction [6] for the case of iron-EDTA complex [F. Roncaroli et al., *Coordination Chemistry Reviews*, **251**,1903-1930 (2007)].

4

$$Fe^{II}(EDTA) + NO \rightleftharpoons Fe^{II}(EDTA)(NO) \qquad [6]$$
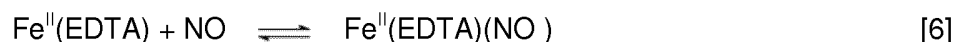
The metal-chelate can be electrochemically regenerated after absorption or reduced
by sulfite ions to sulfate and nitrogen [F. Gambardella et al., *Industrial & Engineering
Chemistry Research* **44**, *4234–4242* (2005)].

In US6235248 a biotechnological approach to regenerate the iron-complex, the so-
called BioDeNO$_x$ process was described. In this process the NO-saturated iron-chelate
solution is brought in close contact with bacteria that regenerate the iron-EDTA
complex and convert the bound nitrosyl to N$_2$. The Fe^{II}(EDTA) solution needs to be
somewhat diluted (concentration <200 mM) due to the presence of microorganisms,
which naturally limits the absorption capacity.

The above proposed technologies for NO removal are all associated with various
challenges such as low capacity, large installation footprint, poor reaction kinetics,
hazardous stoichiometric reductants or oxidants, elevated reaction temperatures and
the requirement for specialized catalysts.

Many of the above proposed technologies are based on liquids with a vapour
pressure, which means that the solvent to some extent vaporizes during operation.

One promising solution to this particular problem could be the use of solvents referred
to as ionic liquids (ILs). The expression 'ionic liquid' in principle encompasses any
liquid entirely composed of ions (e.g. molten salts). However, within the context of this
work the term will only be used to describe materials which are liquid in their pure state
at room temperature. This class of solvents is often considered as 'green' solvents
because of their immeasurably low vapour pressure. This feature gives the ILs an
essential advantage over traditional solvents used for absorbing gases. Ionic liquids
have already demonstrated promising behaviour in a number of reactions where
gaseous reactants enter the IL solution (such as hydrogenation, hydroformylation, and
oxidations) despite low gas solubilities of the gases in the IL at ambient conditions [J.
L. Anthony et al. *The Journal of Physical Chemistry B*, **106**. *7315–7320* (2002)].

5

Another known application of ILs is to utilize them to separate gas mixtures. WO 2007/101397 discloses gas purification processes and mentions a broad range of ionic liquids as possible absorbers of many different gasses, but does not provide any experimental evidence supporting these propositions. WO 2007/101397 is instead

5   merely a theoretical review since there is no data evidencing how the ionic liquids work.

A promising solid ionic cation (1,1,3,3-tetramethylguanidinium) has been identified for the absorption of SO_2 [J. Huang et al., *Journal of Molecular Catalysis A: Chemical*,

10   **279**, *170-176* (2008)]. Similarly, the solubilities of a number of gases (such as CO_2, CO, O_2) in imidazolium-based ILs has been reported by Anthony et al. [J. L. Anthony et al., *The Journal of Physical Chemistry B*, **106**, *7315–7320* (2002)].

Ionic liquids tend to be more viscous compared to conventional solvents, which can

15   result in challenges regarding the mass transfer of gas into the IL. In the case of low-soluble gases, the mass transfer into the IL will likely be a rate limiting step, which can be minimized by increasing the interfacial gas-IL area and/or use high pressure systems [J. L. Anthony et al., *The Journal of Physical Chemistry B*, **106**, *7315–7320* (2002)].

20

Only limited information regarding the gas solubilities in ILs has been reported. Besides the reports regarding CO_2 capture, the focus of most work revolves around the reactions taking place in the IL with the gas already absorbed. Only few reports exist on gas solubilities [J. L. Anthony et al., *The Journal of Physical Chemistry B*, **106**,

25   *7315–7320* (2002); J. L. Anderson et al., *Accounts of Chemical Research*, **40**, *1208–1216* (2007)]. The Brennecke group has, e.g. contributed with a number of seminal studies on absorption of a number of gases in imidazolium-based ILs [J. L. Anthony et al., *The Journal of Physical Chemistry B*, **106**, *7315–7320* (2002); J. L. Anderson et al., *Accounts of Chemical Research*, **40**, *1208–1216* (2007); J. L. Anthony et al., *The*

30   *Journal of Physical Chemistry B*, **105**, *10942–10949* (2001); J. L. Anthony et al., *The Journal of Physical Chemistry B*, **109**, *6366–6374* (2005)].

Consequently, there is still a need for developing efficient and improved processes for removing NO_x, and specifically the most abundant NO_x component NO, from flue

35   gasses from not only large stationary sources like power or incineration plants, but

6

also from mobile emission sources like, e.g. commercial marine vessels which require a small installation footprint and low energy consumption.

Summary of the invention

5   Disclosed herein is a method for removing NO_x gasses by an absorption process and conversion of NO_x to nitric acid (HNO_3) in the presence of oxygen and water, wherein the NO_x gasses comprise NO, NO_2, N_2O_3, and N_2O_5. The NO_x gas can also comprise N_2O_4.

10   The method comprises the step of a) pre-oxidation of nitric oxide (NO) to nitrogen dioxide (NO_2) and other $H_xN_yO_z$ species by use of an ionic composition catalyst at an oxidation temperature below the decomposition temperature of the ionic composition catalyst, thereby forming a pre-oxidized gas mixture. For $H_xN_yO_z$, x, y and z are integers in the ranges x= 0-1, y=1-2, z=1-5. The ionic composition catalyst comprises
15   one or more ionic compounds.

The method further comprises the step of b) absorption of NO_2 and other $H_xN_yO_z$ species generated in the pre-oxidation process of step a) and conversion of the absorbed NO_2 and other $H_xN_yO_z$ species to form nitric acid (HNO_3) wherein the
20   absorption and conversion occurs in a medium in the presence of oxygen and water at an absorption/conversion temperature which is lower than the pre-oxidation temperature in step a) which accumulates in the medium.

Normally, NO_x is removed from polluted air, exhaust gas, combustion gasses, e.g. of a
25   combustion engine, gasses from a chemical reactor and similar. These gasses are sometimes referred to as off-gasses.

Using a two-step process including a pre-oxidation step provides a significantly more effective total reaction. The pre-oxidized gas mixture is more readily absorbed in the
30   second step giving a significantly faster and more efficient conversion into to nitric acid. The nitric acid formed can be collected when regenerating the absorber, thus transforming the pollutant into a product of commercial value. By the present method, a different strategy to remove NO and NO_2 from a gas stream is presented, actively utilizing the water and oxygen present in the flue gas to chemically convert the NOx
35   into nitric acid, HNO_3, which then accumulates in the IL due to the formation of strong

hydrogen bonds. Absorption of NO from the simulated flue gas has been determined to have a second order dependence on NO. This second order dependence is a disadvantage, especially with a dilute reaction component. By pre-oxidizing the gas prior to absorption the reaction order in NOx likely becomes lower than 1, since

5   conversion of NO_2 to HNO_3 can be facilitated solely by water (see reaction scheme below).

$$3\,NO_2 + H_2O \;\rightarrow\; 2\,HNO_3 + NO$$
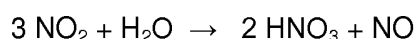
10   In the case of the IL, this reaction occurs differently, primarily forming HONO and HNO_3 in a 1:1 ratio, as is exemplified by the reaction scheme below.

$$2\,NO_2 + H_2O \;\rightarrow\; HNO_3 + HNO_2$$
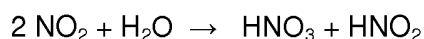
15   The above reaction is part of the catalytic cycle for the oxidation of NO to HNO_3 in ILs. Not having to perform the oxidation to near the same extent should significantly decrease the reaction order in NO, maybe even as low as below one. A such decrease in reaction order by the numerical value of one will under the conditions present in a flue gas, increase the reaction rate for the absorption by several orders of magnitude.

20

The in situ Attenuated Total Reflectance Fourier Transform Infrared (ATR-FTIR) spectroscopic results presented here shows interaction between a thin IL film and a combined gas stream containing dilute NO gas, atmospheric air and water. From time-resolved experiments we have extracted mechanistic evidence for the pre-oxidation

25   and absorption reactions as well as the stoichiometry, kinetics and mechanism of the absorption.

Brief description of the figures

Figure 1 shows the kinetic data suggesting that the reaction rate is second order with

30   respect to NO.

Figure 2 shows the FT-IR spectra of $[BMIM]CH_3COO$ at different exposure times.

Figure 3 shows the FT-IR spectra of [BMIM]Cl at different exposure times.

35

Figure 4a shows the FT-IR spectra of [BMIM]NO$_3$ at different exposure times, figure 4b shows the FT-IR spectra of [BMMIM]NO$_3$ at different exposure times under anaerobe conditions and figure 4c shows the FT-IR spectra of [BMMIM]NO$_3$ mixed with HNO$_3$ at different molar ratios.

Figure 5 shows the FT-IR spectra of [BMMIM]NO$_3$ at different exposure times.

Figure 6 shows the FT-IR spectra of [EMIM]CF$_3$SO$_3$ at different exposure times exposed to a gas stream containing NO (6% v/v), O$_2$ (8% v/v) and water (~1% v/v).

Figure 7 shows the FT-IR spectra of [choline]CH$_3$COO at different exposure times.

Figure 8 shows the FT-IR spectra of [choline]NO$_3$ at different exposure times.

Figure 9 shows the FT-IR spectra of 1,2,3,4-tetramethyl-guanidinium chloride at different exposure times.

Figure 10 shows the observed amount of HNO$_3$ per mol IL for different ionic composition catalysts.

Figure 11 shows the absorption of NO performed on bulk [BMIM]CH$_3$COO with 10% NO in N$_2$ being bubbled through 1 g of IL.

Figure 12 shows the TGA data.

Figure 13 shows the ^{1}H data in CDCl$_3$ of [BMIM]acetate after NO absorption and desorption. No peaks from acetate or acetic acid are discernible (CH$_3$ group of acetate has a peak at 2.10 ppm in CDCl$_3$).

Figure 14 shows the ^{13}C NMR data of [BMIM]acetate. No peaks from acetate or acetic acid are discernible (CH$_3$ group of acetate has a peak at 20.81 ppm, COO$^-$ group of acetate has a peak at 175.99 ppm in CDCl$_3$).

Figure 15 shows the symmetric and antisymmetric N-O stretch modes of the HNO$_3$ dimer.

9

Figure 16 shows an ATR-FTIR spectrum of [BMIM][NO$_3$] exposed to a gas stream containing NO$_2$. The dotted line corresponds to the spectrum of pure IL in equilibrium with the atmosphere, the grey lines to the spectra recorded after NO$_2$ exposure for 3

5   min and the black line to the spectrum recorded after subsequent 30 s of exposure to N$_2$ saturated with water. Bands from BMIM+, N$_2$O$_4$, NO$_3^-$, HNO$_3$ and HONO are indicated.

Figure 17 shows ATR-FTIR spectra showing [BMIM]NO$_3$ prior to exposure (solid black

10   line) and after exposure to a mixture of NO 10% v/v, H$_2$O 2% v/v and balance N$_2$. The spectra are identical apart from a slight increase in water concentration (band at 3500 cm-1), causing a slight decrease in the free nitrate signal (band at 1340 cm-1) due to hydrogen bonding.

15   Figure 18 shows relative rate of HNO$_3$ formation in [BMIM][NO$_3$] with 2 % v/v NO with excess water and oxygen at different temperatures. A dotted line is added as a guide to the eye. Rates are determined as the maximal linear rate of the change in intensity of the 948 cm-1 band in the in-situ ATR-FTIR spectra.

20   Figure 19 shows UV-Vis spectrum showing oxidation of NO to form NO$_2$. A SILP catalyst (30% porefilling, BMIM NO$_3$ on uncalcinated silica (Saint Gobain SS138)), situated in a fixed bed reactor with a temperature of 70°C was exposed to a continuous flow of simulated flue gas containing 900 ppm H$_2$O, 2000 ppm NO, 15% O2 and balance N$_2$.

25
Figure 20 shows concentration profiles corresponding to the spectra presented in figure 19.

Figure 21 shows UV-Vis spectrum showing oxidation of NO to higher NOx species. A

30   SILP catalyst (30% pore filling, BMIM NO3 on calcinated anatase (Saint Gobain ST120)), situated in a fixed bed reactor with a temperature of 90°C and 120°C was exposed to a continuous flow of simulated flue gas containing 1% H$_2$O, 2000 ppm NO, 15% O$_2$ and balance N$_2$.

35   **Detailed description of the invention**

In an aspect of the invention, a method for removing NO_x gasses by an absorption process and conversion of NO_x to nitric acid (HNO_3) in the presence of oxygen and water, wherein the NO_x gasses comprise NO, NO_2, N_2O_3 and N_2O_5. The NO_x gas can also comprise N_2O_4.

The method comprises the step of a) pre-oxidation of nitric oxide (NO) to nitrogen dioxide (NO_2) by use of an ionic composition catalyst at an oxidation temperature below the decomposition temperature of the ionic composition catalyst, thereby forming a pre-oxidized gas mixture. In the pre-oxidation step, other $H_xN_yO_z$ species may also be formed in addition to NO_2, where x, y and z are integers in the ranges x= 0-1, y=1-2, z=1-5. Normally NO_2 will be the dominant species generated in the pre-oxidation process however, step a) may also include pre-oxidation of nitric oxide (NO) to nitrogen dioxide (NO_2) and other $H_xN_yO_z$ species by use of an ionic composition catalyst at an oxidation temperature below the decomposition temperature of the ionic composition catalyst.

The method further comprises the step of b) absorption of NO_2 and other $H_xN_yO_z$ species generated in the pre-oxidation process of step a) and conversion of the absorbed NO_2 and other $H_xN_yO_z$ species to form nitric acid (HNO_3) wherein the absorption and conversion occurs in a medium in the presence of oxygen and water at an absorption/conversion temperature which is lower than the pre-oxidation temperature in step a) which accumulates in the medium.

The ionic composition catalyst may preferentially comprise one or more ionic compounds.

In one or more embodiments, the medium is an ionic composition absorber comprising one or more ionic compounds.

In one or more embodiments, the ionic composition absorber is different from the ionic composition catalyst.

In one or more embodiments, the ionic composition absorber is identical to the ionic composition catalyst.

11

In one or more embodiments, the ionic composition catalyst is adjusted in volume and/or flow rate to obtain a high conversion of NO to NO_2 and other $H_xN_yO_z$ species in the pre-oxidized gas mixture before performing step b).

5

In one or more embodiments, the conversion of NO to NO_2 and other $H_xN_yO_z$ species is more than 50%.

In one or more embodiments, the conversion of NO to NO_2 and other $H_xN_yO_z$ species
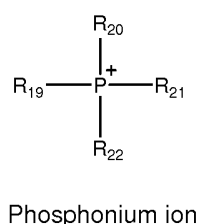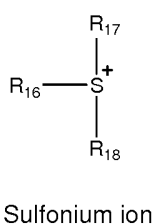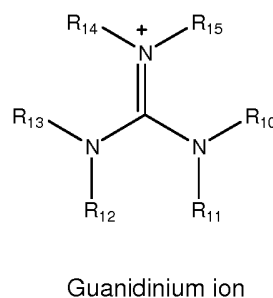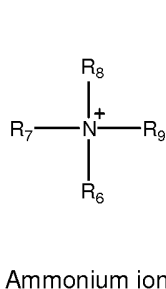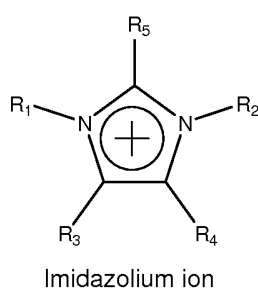
10   is more than 60%.

In one or more embodiments, the conversion of NO to NO_2 and other $H_xN_yO_z$ species is more than 70%.

15   In one or more embodiments, the conversion of NO to NO_2 and other $H_xN_yO_z$ species is more than 80%.

In one or more embodiments, the conversion of NO to NO_2 and other $H_xN_yO_z$ species is more than 90%.

20

In one or more embodiments, the conversion of NO to NO_2 and other $H_xN_yO_z$ species is a full conversion.

In one or more embodiments, the pre-oxidation temperature in step a) is between 70

25   and 200°C, between 75 and 150°C, or between 80 and 120°C. In one embodiment the pre-oxidation temperature in step a) is between 20 and 200°C, or between 40 and 200°C, or between 20 and 150°C, or between 30 and 120°C, or between 30 and 100°C, or between 30 and 50°C, or between 40 and 50°C.

30   In one or more embodiments, the absorption/conversion temperature in step b) is between 20 and 120°C, between 25 and 100°C, or between 30 and 80°C.

In one or more embodiments, the one or more ionic compounds in the ionic composition catalyst and/or the ionic composition absorber comprising one or more

35   organic cations selected from:

12

R5

R1—N(+)N—R2

R3   R4

Imidazolium ion

R8

R7—N(+)—R9

R6

Ammonium ion

R14   +   R15
      N

R13—N   N—R10

R12   R11

Guanidinium ion

R17

R16—S(+)

R18

Sulfonium ion

R20

R19—P(+)—R21

R22

Phosphonium ion

wherein

- R1, R2, R3, R4, R5, R6, R7, R8, R9, R10, R11, R12, R13, R14, R15, R16, R17, R18, R19, R20, R21 and R22 can be, independently, hydrogen, alkyl, halogenated alkyl, aminoalkyl, hydroxyalkyl, alkoxyalkyl, alkenyl, alkynyl, aryl, heteroaryl, cycloalkyl, cycloalkenyl, heterocycloalkyl, or heterocycloalkenyl;

- the positively charged P, N and S atoms may individually be part of heterocyclic or heteroaromatic structures by letting:

  • two of R20, R21, R22, R23, e.g. R21 and R22 be fused such that a cyclic phosphonium ion is formed; or

  • two of R6, R7, R8, R9 eg. R6 and R7 be fused, such that a cyclic ammonium ion is formed, such as a pyridinium ion; or

  • two of R11 and R12, R13 and R14, R15 and R10,eg. R11 and R12 be fused, such that a cyclic guanidinium ion is formed; or

  • two of R16, R17 and R18 eg. R16 and R17 be fused, such that a cyclic sulfonium ion is formed;

- optionally one or more cations selected from inorganic cations such as Li^+, Na^+ and K^+, and

- one or more anions selected from C_1-C_6 alkanoates such as acetate, arylcarboxylates such as benzoate, C_1-C_6 alkylsulfates such as ethyl sulfate, C_1-C_6 alkylsulfonates, C_1-C_6 perfluoroalkylsulfonates such as triflate, C_1-C_6 perfluoroalkanoates such as trifluoroacetate, C_1-C_6 perfluoroalkylsulfonimides such as bis(trifluoromethylsulfonyl) imide (triflic imide), tetrafluoroborate, hexafluorophosphate, sulfate, nitrate and halides such as chloride or bromide.

In one or more embodiments, the one or more ionic compounds in the ionic composition catalyst and/or the ionic composition absorber comprising a cation having the following structure:

5

wherein R_1 and R_2 are individually selected from C_1-C_8 alkyl groups or aryl groups, and wherein R_3, R_4 and R_5 are individually selected from hydrogens, C_1-C_6 alkyl groups or aryl groups or wherein R_3 and R_4 together with the imidazolium group may form a 4- to 6-membered saturated, unsaturated or aromatic ring, which may further contain up to

10   three hetero atoms selected from oxygen, nitrogen and phosphorus.

In one or more embodiments, the one or more ionic compounds in the ionic composition catalyst and/or the ionic composition absorber comprising a cation selected from: BMIM = 1-butyl-3-methylimidazolium, EMIM = 1-ethyl-3-

15   methylimidazolium, BMMIM = 1-butyl-2,3-dimethylimidazolium, choline = N-(2-hydroxyethyl)-N,N,N-trimethylammonium.

In one or more embodiments, the one or more ionic compounds in the ionic composition catalyst and/or the ionic composition absorber is selected from 1-ethyl-3-

20   methylimidazolium ($[EMIM]^+$) acetate, 1-butyl-3-methylimidazolium ($[BMIM]^+$) acetate, 1-ethyl-3-methylimidazolium ($[EMIM]^+$) triflate, 1-butyl-3-methylimidazolium ($[BMIM]^+$) triflate, 1-ethyl-3-methylimidazolium ($[EMIM]^+$) nitrate, 1-butyl-3-methylimidazolium ($[BMIM]^+$) nitrate, 1-butyl-2,3-dimethylimidazolium ($[BMMIM]^+$) nitrate, choline chloride, choline acetate and 1,1,3,3-tetramethylguanidinium chloride.

25

In one or more embodiments, the ionic composition catalyst and/or the ionic composition absorber further comprises one or more cations selected from Li^+, Na^+ and K^+.

14

In one or more embodiments, the ionic composition catalyst and/or the ionic composition absorber contains a non-ionic solvent.

In one or more embodiments, the ionic composition catalyst and/or the ionic
5   composition absorber contains a solid material.

In one or more embodiments, the one or more ionic compounds in the ionic composition catalyst is an ionic liquid.

10   In one or more embodiments, the one or more ionic compounds in the ionic composition absorber is an ionic liquid.

In one or more embodiments, the ionic composition catalyst and/or the ionic composition absorber is dispersed on a porous carrier and used in the form of a
15   supported ionic composition phase material

In one or more embodiments, the ionic composition catalyst and/or the ionic composition absorber is an ionic liquid dispersed on a porous carrier and used in the form of a supported ionic liquid phase (SILP) material.
20
Supported Ionic Liquid Phase (SILP) materials consist of an ionic liquid distributed over a porous support material with a high surface area. SILP materials are particularly useful for reactions involving gas phase reactants and may be used as catalysts, where the ionic liquid is the catalytically active component itself or is used to dissolve
25   catalytically active components in the ionic liquid phase, or as gas absorbers. Since most ILs are highly viscous, simply bubbling a gaseous reactant through the liquid leads to an insufficient substance transport over the phase boundary due to the large bubble size and slow diffusion in the liquid phase. The SILP formulation eases diffusion, since the available surface area becomes much larger.
30
IL and/or SILP materials provide high thermal stability, low vapor pressures and high electronic and proton conductivities.

In one or more embodiments, the porous carrier material is composed of carbon, zeolites, clays, hydroxides or oxides based on the elements Si, Al, Ti, Ce, Zr, Mg, Fe, Ca, Sr, Ba, Mn, Ge and/or Ga.

5   In one or more embodiments, the porous carrier material is selected from SiO_2, Al_2O_3, TiO_2, CeO_2, ZrO_2, carbon or a combination of two or more of these.

In one or more embodiments, the porous carrier material is TiO_2, e.g. anatase TiO_2.

10   The porous carrier material may be crushed and fractioned to obtain particles e.g. of sizes from 180 - 355 µm.

In one or more embodiments, a wet scrubbing system for removal of SO_2 and SO_3 comprised in the off-gasses is implemented before performing step a).

15

In one or more embodiments, the off-gasses are flue gases originating either from large stationary sources like power or incineration plants or cement production plants, or from mobile emission sources like e.g. commercial marine vessels or mobile incineration plants for incineration of e.g. domestic or industrial waste.

20

Throughout the present application, if not otherwise specified, 'incineration plant' shall mean any stationary or mobile technical unit and equipment dedicated to the thermal treatment of wastes with or without recovery of the combustion heat generated. This includes the incineration by oxidation of waste as well as other thermal treatment

25   processes such as pyrolysis, gasification or plasma processes in so far as the substances resulting from the treatment are subsequently incinerated.

NO removal in mobile units, such as commercial marine vessels and mobile incineration units for e.g. domestic or industrial waste represent other relevant

30   examples for considering the implementation of the reversible ionic compositions system of the present invention because of the much less hazardous reaction conditions, lower reaction temperatures and smaller installation footprint.

Throughout the present application, if not otherwise specified, off-gasses is to be understood as any gas emitted leading to air pollution as exhaust or combustion gasses, e.g. of a combustion engine or a chemical reactor and similar.

5   Throughout the present application, if not otherwise specified all nitrogen dioxide species, including dimers thereof, are considered as chemical NO_2 and are thus referred to as NO_2 in argumentation and reactions.

The reaction converting NO to HNO_3 when NO is in the presence of oxygen and water
10   is thermodynamically favored with $\Delta_r G = -210$ kJ mol^{-1}.

$$4 \text{ NO (g)} + 3 \text{ O}_2\text{(g)} + 2 \text{ H}_2\text{O (l)} \rightarrow 4 \text{ HNO}_3\text{(l)} \tag{7}$$
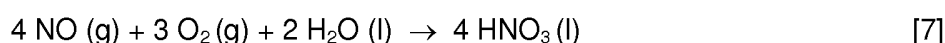
Kinetically, however, the reaction in reaction scheme [7] is very hindered. NO is a
15   relatively unreactive molecule but will easily react once activated. The base-strength of the anion in the ionic liquid is believed to be important in providing this activation of NO. The kinetic data shown in figure 1 shows a plot of the logarithmic relative reaction rate (R) as a function of the logarithmic concentration. The equation for the linear trend line is also shown in the figure and points clearly to the reaction being second order in
20   NO.

The oxidation of NO to NO_2 in the gas phase and to H^+ / NO_2^- in the aqueous phase has the same rate law, as described below:

25           $$-\frac{d[\text{NO}]}{dt} = k[\text{NO}]^2[\text{O}_2] \tag{8}$$

This is despite the total reactions for gas phase (reaction scheme [9]) and for aqueous solution (reaction scheme [10]) being rather different as shown below.

30           $$2 \text{ NO (g)} + \text{O}_2\text{(g)} \rightarrow 2 \text{ NO}_2\text{(g)} \tag{9}$$
             $$4 \text{ NO (g)} + \text{O}_2\text{(g)} + 2 \text{ H}_2\text{O (l)} \rightarrow 4 \text{ H}^+\text{(aq)} + 4 \text{ NO}_2^-\text{(aq)} \tag{10}$$
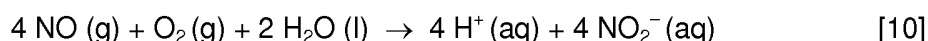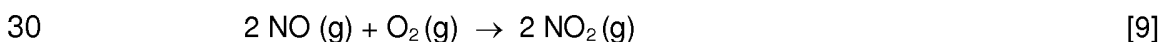
A second order dependence on the concentration of NO(g) over an ionic liquid (IL) film was observed. Thus, the same rate law is also expected to be relevant for the rate-
35   determining step in ionic liquid solution.

17

A first step in the condensed ionic liquid phase obeying the second order rate law
could be:

5
$$NO\ (g) + NO_3^-\ (IL)\ \rightleftarrows\ N_2O_4^-\ (IL)$$ [11]
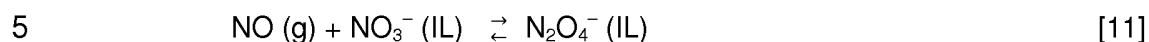
Nitrate (NO_3^-) is a much more powerful base and nucleophile in the ionic liquid phase
than in normal aqueous solution allowing it to attack the kinetically inert NO gas
molecule. The unstable adduct then decomposes to nitrogen species in the
10   intermediate oxidation steps:

$$N_2O_4^-\ (IL)\ \rightleftarrows\ NO_2\ (IL) + NO_2^-\ (IL)$$ [12]
$$2\ NO_2\ (IL)\ \rightleftarrows\ N_2O_4\ (IL)$$ [13]

15   In the majority of the described experiments water is purposely provided to the
reaction. The second part in the reactions for converting NO to HNO_3 is therefore
envisioned to proceed through the following steps:

$$N_2O_4\ (IL) + H_2O\ (IL)\ \rightarrow\ HNO_3\ (IL) + HNO_2\ (IL)$$ [14]
20

$$HNO_2\ (IL) + NO_2^-\ (IL)\ \rightleftarrows\ \text{``}HN_2O_4^-\text{''}\ (IL)$$ [15]
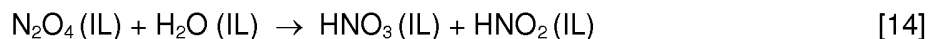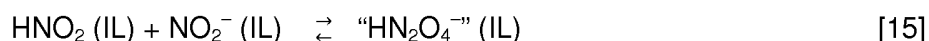
The last dimeric species formed in reaction [15] is simply bonded by a strong hydrogen
bond holding the two N(III) species close together and activating them for oxidation by
25   dioxygen in one step. The product is the analogous nitrate-nitric acid dimer ("$HN_2O_6^-$"):

$$\text{``}HN_2O_4^-\text{``}\ (IL) + O_2\ (IL)\ \rightarrow\ \text{``}HN_2O_6^-\text{''}\ (IL)$$ [16]
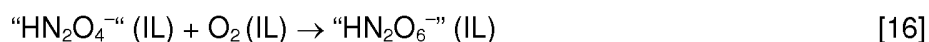
The nitrate-nitric acid dimer is clearly observable in the IR spectrum of [BMIM]NO_3 (1-
30   butyl-3-methylimidazolium nitrate) shown in figure 4a as the peaks at 1296 and 1420
cm^{-1}. The nitrate-nitric acid dimer is the final product until the nitric acid is desorbed by
increasing the temperature as shown in reaction [17]:

$$\text{``}HN_2O_6^-\text{''}\ (IL)\ \rightarrow\ HNO_3\ (g) + NO_3^-\ (IL)$$ [17]
35

18
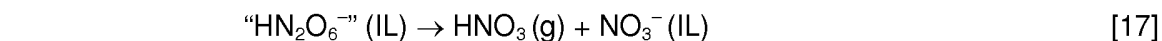
The suggested complete reaction pathway is shown in the catalytic cycle below. Here, the total reaction for the oxidation of NO to HNO_3 catalyzed at RT by nitrate based ILs is shown.
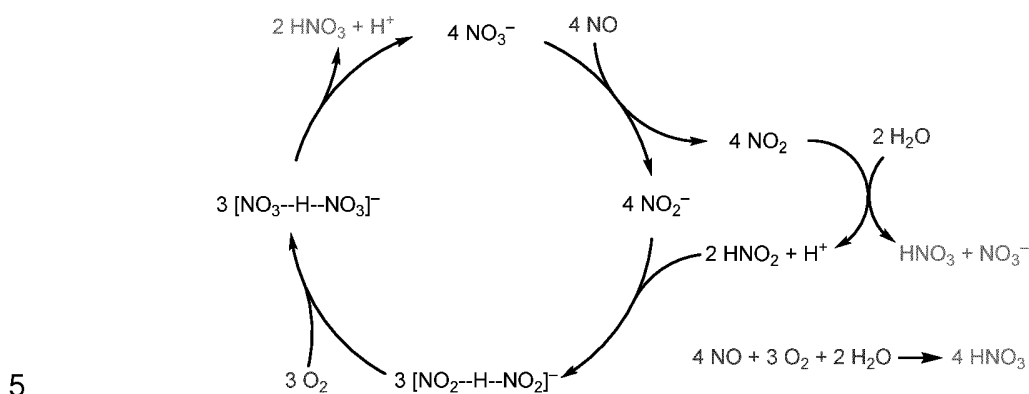
As seen from the proposed reaction pathway, we believe that radicals originating from dioxygen are not formed during the turnover of the reaction. The fact that the organic cations are unaffected by the harsh treatment is also a strong indication that the formation of uncontrollable reactive radical species is suppressed in the IL media. Any other, less protected, organic molecules or particles present in the IL are likely oxidized and decomposed completely to CO_2 and water giving a self-cleaning process of the IL during heating to the regeneration temperature.

The ILs with anions which are stronger bases than nitrate will be converted to the nitrate IL after one cycle where the corresponding acid is expelled. For example, acetate is a very powerful base in an IL and if an experiment is performed on [BMIM]CH_3COO (1-butyl-3-methylimidazolium acetate), the IR features assignable to acetate decrease rapidly and acetic acid can be seen in the IR spectrum of [BMIM]CH_3COO as shown in figure 2. The band assignable to acetic acid quickly disappears, suggesting that the acid is expelled from the IL. Simultaneously, the anion changes towards the nitrate-nitric acid dimeric species discussed above. The new anion changes the physical properties of the IL drastically since [BMIM]NO_3 (see figure 4) has a much lower viscosity and a higher thermal stability than [BMIM]CH_3COO, see figure 13 showing the TGA data.

Acetic acid is volatile and is easily expelled from the IL under flow conditions, leaving the [BMIM]NO_3 to perform further oxidation and absorption. A similar situation is seen

for [BMIM]Cl (1-butyl-3-methylimidazolium chloride) since chloride is also a stronger base than nitrate in the IL and HCl – a gas – will desorb readily from the ionic liquid. The IR spectra of [BMIM]Cl at different times after NO exposure is shown in figure 3 and shows the buildup of HNO_3 observed as the bands at 940 cm^{-1} and 1660 cm^{-1}.

Figure 6 regarding [EMIM][CF$_3$SO$_3$] shows that the oxidation reaction still proceeded forming HNO_3, but slower than with the acetate, nitrate- and chloride-based ILs. Notably, the strong bands from nitrate was not observed after desorption, whereas the strong bands originating from the triflate anion were observed throughout the experiment. The latter bands only changed moderately after accumulation of HNO_3 in the IL, suggesting that hydrogen bonding of HNO_3 to the anion was present but less pronounced than observed in the experiments with the nitrate IL. Hence, the strong triflate band centered at 1270 cm^{-1} (antisym. S=O stretch) lost intensity and broadened when HNO_3 was present but regained intensity after desorption.

In order to probe the influence of the cation on the reaction, and to determine if the observed uptake was due to reaction with the C2 position of the cation, [BMIM]$^+$ was exchanged for [BMMIM]$^+$ (1-butyl-2,3-dimethylimidazolium) possessing an extra methyl group in the C2 position on the imidazolium ring. Comparing the IR spectra of [BMIM]NO$_3$ at different times after NO exposure in figure 4a with the IR spectra of [BMMIM]NO$_3$ at different times after NO exposure in figure 5, it can be seen that the additional methyl group makes little difference on the absorption rate and total capacity. This can also be seen in figure 10 displaying the observed amount of HNO_3 per mol IL. In figure 10, there is a small difference in the reaction rates, however this is likely due to the [BMIM]NO$_3$ experiments being performed at a later point in time, where the method had been optimized to better study the reaction kinetics. The term [BDMIM] is used interchangeably with [BMMIM]. Acetate is the strongest base and the corresponding acid (acetic acid) is easily driven off giving a curve identical to the one for [BMIM]nitrate.

In order to assess the importance of the imidazolium ring, the simpler, biodegradable and nontoxic choline cation was used. This posed some problems in the quantification since IR peaks from the cation are found at the same positions as one of the quantifiable HNO_3 bands. The same trends as described above are also seen in figure 7, showing the IR spectra of choline acetate ((2-hydroxyethyl)trimethylammonium)

acetate) at different times after NO exposure. As with the [BMIM] based ILs, oxidation of NO and subsequent absorption of the end product, HNO_3, is observed. Upon regeneration of the IL facilitated by heating, the nitrate IL is observed as the only product. The reaction intermediates observed during reaction are consistent with the ones observed during reaction with [BMIM] based ILs, presented in the catalytic cycle above. Thus it can be concluded that the chosen cation has no apparent influence on the observed reaction rate nor the reaction mechanism.

The rate of accumulation of nitric acid in the IL is very dependent on the NO concentration and also on the temperature as can be seen in figures 1 and 19. At room temperature and 6% v/v NO, the reaction proceeded quickly, and saturation was obtained after only 50 seconds. At 1 % v/v NO it took more than 3000 seconds before saturation was obtained, in good accordance with the reaction being second order in NO. A second order reaction in NO is far from optimal, given that most flue gasses contain 300-1000 ppm of NO_x (often in the low end). The rate equation for formation of nitric acid is described in the below equation:

$$r = k * [NO]^2 * \left[O_2\right] = k * p_{NO}^2 * p_O$$

As is seen from the rate equation, a second order dependence means that the NO concentration is squared. This gives a sharp decrease in HNO_3 formation with decreasing NO concentration.

By preoxidizing the NO, the reaction order for the rate determining absorption step can be reduced, thus increasing the reaction rate significantly at lower concentrations. The spontaneous reaction between water and NO_2 to form nitric acid is used e.g. in the Ostwald process to produce nitric acid on an industrial scale. The reaction proceeds as: $NO_2 + H_2O \rightarrow HNO_3 + HNO_2$, and is facilitated by liquid water present in the reactor. The IL is an excellent facilitator for this reaction, which is seen from figure 16. Here, the IL has been exposed to pure, dried NO_2 gas. The IL still contained some water, resulting in almost instantaneous formation of nitric acid, as seen from the bands at 940 cm^{-1} and 1660 cm^{-1}. Bands assignable to N_2O_4 are also present in high amounts, suggesting that water is a limiting factor.
After a couple of minutes, the IL was exposed to an N_2 gas saturated with water. This resulted in further formation of nitric acid, while the concentration of N_2O_4 decreased

significantly. The bands assignable to HONO follows the HNO_3 bands, strongly
suggesting that the following reaction takes place:

$$2 NO_2 + H_2O \rightarrow \quad HNO_3 + HNO_2 \qquad \qquad [18]$$

5

The accumulation of HONO (HNO_2) suggests that oxygen became the limiting factor
once water was provided, as expected. The intensity of the nitric acid bands show that
a large amount of HNO_3 can be formed without performing the rate-limiting oxidation,
when the NO_x is provided as NO_2 or higher NO_x species. Thus, the rate equation will

10   change and the dependency on NO_x concentration will decrease significantly, likely to
or below 1.
A decrease in reaction order under the low concentrations found in a flue gas, will
increase the reaction rate by several orders of magnitude. As an example; if the NO_x
concentration is 500 ppm and the reaction order in NO_x is 1 instead of 2, the rate of

15   formation for HNO_3 would increase by 2000.
When the IL is exposed to NO and water in the absence of oxygen, no reaction occurs,
further underlining the importance of pre-oxidation. This can be seen from figure 17, in
which the IL was exposed to a wet mixture of NO and water for more than an hour
without any reaction occurring. This is opposed to significant reaction occurring after

20   30 seconds with NO_2.

Increasing the temperature slightly is expected to also increase the rate of the limiting
oxidation reaction. Figure 18 shows the effect of increasing the temperature slightly.
As can be seen from figure 18, there is a large gain from doing so, starting out. At

25   higher temperatures the rate decreases again, suggesting that another factor becomes
rate limiting. This factor is likely solubility of the gaseous species in the IL, which
decreases with temperature. Thus, the reaction can be improved drastically by
performing the oxidation at higher temperatures, while having a low temperature
absorption bed, in which the solubility is improved.

30

Protons are being formed in the oxidation reaction and since the proton conductivity is
very high in ionic liquids they might quickly be led away from the surface. When the IL
is saturated with HNO_3 there are just enough protons to allow every proton to form a
strong hydrogen bond between two nitrate anions. This is also supported by the

35   observation that no water is accumulated in the IL after saturation.

Figure 19 shows the UV-Vis spectra for oxidation of NO to form NO_2. A SILP catalyst
(30% porefilling, BMIM NO3 on uncalcinated silica (Saint Gobain SS138)), situated in
a fixed bed reactor with a temperature of 70°C was exposed to a continuous flow of

5   simulated flue gas containing 900 ppm H_2O, 2000 ppm NO, 15% O_2 and balance N_2.
The broad band with maximum at 210 (215) nm is characteristic for NO_2 and increases
with time, thus indicating that a significant amount of NO_2 is formed. After 30 minutes,
steady state is reached. The continuous conversion of NO at steady state corresponds
to around 70%, based on the characteristic NO peak at 119 (124) nm. The numbers

10   presented in parentheses correspond to the table values for the species. The deviation
from table values is caused by a constant instrument effect. There is a significant
activation period where no significant NO oxidation is observed. After this induction
period, the conversion appears to remain constant.

15   Figure 20 shows the concentration profiles corresponding to the spectra presented in
figure 19. The concentrations have been determined for NO by deconvolution of the
spectral information, using the same method as presented earlier. UV/VIS
spectroscopy is not optimal for quantification of NO_2, however, no trace of other NOx
species was observed. Therefore, it is assumed that the NO_2 concentration can be

20   determined from the NO conversion; ($[NO_2]$ = 2000 ppm – $[NO]$). This assumption is
further justified by looking at the spectral data, which clearly shows high
concentrations of NO_2.

Figure 21 shows an UV-Vis spectrum showing oxidation of NO to higher NOx species.

25   A SILP catalyst (30% pore filling, BMIM NO3 on calcinated anatase (Saint Gobain
ST120)), situated in a fixed bed reactor with a temperature of 90°C and 120°C was
exposed to a continuous flow of simulated flue gas containing 1% H_2O, 2000 ppm NO,
15% O_2 and balance N_2. At 90°C, the primary oxidation product is NO_2, as can be
seen from the broad band with maximum at 210 (215) nm. At 120°C, formation of

30   another NOx species is observed, while the concentration of NO_2 seems to decrease.
The NOx species has a broad peak with a peak maximum at an estimated 190 (195)
nm, corresponding to that of N_2O_5. The peak maximum of this new NOx species can
only be estimated as it is just outside the spectral range. The continuous conversion of
NO at 120°C corresponds to around 35%, based on the characteristic NO peak at 119

35   (124) nm. At 90°C, this number is around 20%. The numbers presented in

parentheses correspond to the table values for the species. The deviation from table values is caused by a constant instrument effect.

The ILs do not decompose even when heated above 120° in concentrated nitric acid.

5   The original IR spectrum of the IL is completely recovered after cooling to room temperature even after many cycles if the gas stream contains water, as can be seen in figures 4, 5, 6, and 8. If kept completely dry and warm for longer periods some yellow coloration is observed, but the IL still absorbs NO subsequent runs.

10   The imidazolium ring is well protected from electrophilic attack of NO_2^+ or similar species by the positive charge on the imidazolium ring. As seen from the proposed reaction pathway, radicals originating from dioxygen are not expected to form during the reaction – at least not under the conditions used here. The fact that the organic cation survives the harsh treatment is a strong indication that the formation of

15   uncontrollable reactive radical species is suppressed in the ionic liquid media.

The absorption of NO has also been performed on bulk [BMIM]CH_3COO and [BMIM]NO_3. For the [BMIM]CH_3COO 10% v/v NO in N_2 was bubbled through 1 g of IL resulting in the gravimetric data shown in figure 11. For the [BMIM]NO_3, water and air

20   was added so the NO concentration was 5% v/v, with 10% v/v O_2 and around 1% H_2O v/v. The reactions were followed gravimetrically and the observations are in accordance with the conclusions drawn from the FTIR data. The weight increase after cooling to room temperature corresponds to 1.3 mol HNO_3 per mol IL. The acetic acid is easily lost as shown by the NMR data in figure 13 and 14. The viscosity and the

25   thermal stability of the IL changed drastically after absorption. See the TGA data in figure 12 for the thermal stability changes.

^{1}H and ^{13}C NMR clearly shows that very acidic protons (13.8 ppm) are present and any signals corresponding to acetic acid or acetate are lost after one heating cycle. This is

30   seen in figure 13 and14.

The FTIR spectroscopic results for running a combined gas stream of dilute NO and atmospheric air saturated with water over a thin film of a series of ionic liquids are show in figure 2 for [BMIM]CH_3COO, figure 3 for [BMIM]Cl, figure 4a for [BMIM]NO_3,

35   figure 5 for [BMMIM]NO_3, figure 6 for [EMIM]CF_3SO_3, figure 7 for [choline]CH_3COO,

24

figure 8 for [choline]NO$_3$ and figure 9 for 1,2,3,4-tetramethyl-guanidinium chloride. The
reactions are followed in real time with FTIR by recording spectra every few seconds.
The different relevant species that can be observed in this experiment are: nitrate
(1340 cm^{-1}), nitric acid (940 cm^{-1} and 1660 cm^{-1}), water (3350 cm^{-1} and 1655 cm^{-1}),

5   acetate (1540 cm^{-1}), and acetic acid (1700 cm^{-1}).

In the experiment with [BMIM]NO$_3$ in figures 4a and 4b, we see an immediate
decrease in the strong band at 1340 cm^{-1} originating from the asymmetric O-N stretch
of the nitrate ion as acidic protons are building up and generating less symmetric

10   species. Within 20 seconds, the characteristic peak of the HNO$_3$ molecule at 940 cm^{-1}
increases as seen in figure 4a. This line corresponds to the symmetric O=N=O
bending mode. Since it remains unchanged if H is substituted for D, it must correspond
to the oxygens not directly bonded to H.

15   The other characteristic peak at 1660 cm^{-1} shifts with deuterium substitution and
corresponds to a combination band consisting of the asymmetric O=N=O stretch
combined with the O-H/D bend. Either of the lines (940 cm^{-1} and 1660 cm^{-1}) can be
used to quantify the amount of HNO$_3$ present in the ionic liquid by Gaussian peak
analysis and integration (not shown here). The results of the line at 940 cm^{-1} were

20   slightly more reproducible, but all conclusions are equally valid from the quantifications
of the 1660 cm^{-1} line. These bands are illustrated in figure 15.

In order to accurately determine the nitric acid concentrations in the IL during raction,
we used standard solutions prepared by dissolving known amounts of concentrated

25   nitric acid in [BMIM]NO$_3$, measuring the IR spectrum and creating a standard curve.
The integrated peaks of the measurement series were then compared in every point
with the standard curve to give the results as molar ratios of HNO$_3$ to IL.

Desorption takes place when the IL is heated above 120°C corresponding well to the

30   boiling point of concentrated aqueous nitric acid of 121°C. The FTIR spectrum of the IL
in figures 5-6 and 8 is unchanged from the original spectrum when returning to room
temperature, except for water content, and a new cycle can be performed. From the
NMR study shown in figure 13 and 14, it is evident that the IL still retains some acidic
protons when only desorbed at 120 °C.

35

The reaction rate of the combined absorption and oxidation was determined from Gaussian fitting performed on ATR-FTIR data. The Gaussian fit was performed using GnuPlot 4.6.

5   The reason for using Gaussian curves is that spectroscopic data stems from quantized intramolecular motions that are distributed almost evenly around a top point. This distribution corresponds somewhat to a Gaussian distribution and can therefore be simulated using Gaussian functions. Once the spectrum is dissolved into its individual components, the area beneath the individual Gaussian curves will correspond to the
10   concentration of that component. The Gaussian fit is performed by iterations, changing one parameter at a time until the difference between the real spectrum and the simulated spectrum is insignificant.

The Gaussian fit was performed in the spectral range from 800 cm^{-1} to 1100 cm^{-1}.
15   Concentration of the nitric acid formed during reaction was determined based on the peak at 940 cm^{-1}.

Experimental details

In-situ ATR-FTIR spectroscopy
20   The FT-IR Measurements was performed on a heatable diamond ATR plate (Pike GladiATR) using a Nicolet iS5 spectrometer. In order to control the atmosphere over the ionic liquid film on the ATR crystal, a stainless steel cap with a heat resistance polymer sealing was constructed. The steel cap was supplied with two fittings of in- and outlet gas. The inside volume of the cap was approximately 2 millilitre (mL). The
25   ATR cell could be heated up to 300 °C. In the first three examples 8 scans with a resolution of 4 cm^{-1} was used to record each spectrum. The duration of each recording was 11 seconds under these conditions. In the later examples, the number of scans was decreased to 4 lowering the recording time to 6 seconds. The spectra were ATR corrected using OMNIC Lite software, assuming a refractive index of 1.5.
30

The iS5 spectrometer as well as the base optics in the Pike ATR cell was purged with nitrogen in order to minimize loss of the signal to gas phase water and carbon dioxide inside the instrument.

Gases used: Argon 99.999%, Nitrogen 99.99999%, 10 vol% nitrogen oxide in nitrogen, and pressurized air. Gases used for the experiments were purchased from AGA. The gas flow was controlled with Bronkhorst mass flow controllers. In experiments with water in the gas, air or argon was bubbled through a glass frit in a flask with distilled

5   water. The resulting water content in the gasses after saturation was calculated to 2.7 vol% from the vapor pressure at room temperature.

Deconvolutions of the ATR-IR spectra were performed with Systat Peakfit 4.12 software using the build in "Residuals" Algorithm. The typical procedure was to fit the

10   steady state spectra with Gaussian curves allowing both width and position of each peak to move. When a good deconvolution was made on the steady state spectra the peak parameters obtained from this deconvolution was saved and used for the next spectra. Now both position and width of each peak was constrained, so only the intensity of the peaks was changed during the following deconvolutions. The

15   concentration of HNO_3 was determined either from integration of the band around 1650 or 940 cm^{-1} after deconvolution. In the case of water in [BMIM]Cl, the broad band at 3400 cm^{-1} was used. To make an absolute estimate of the HNO_3 concentration a standard solution was prepared with concentrated nitric acid (68 vol%) in [BMIM]NO_3. The spectra of the standard solution were fitted using the same peak parameters as

20   for the steady state spectra.

An experimental procedure to measure the NO absorption capacity by weight increase in the ILs can also be employed, wherein preliminary gas absorption is carried out in a ca. 5 ml test tube with 1 ml ionic liquid (IL) at room temperature (22–23°C). The 10

25   vol% NO/N_2 gas mixture is introduced into the IL through a glass Pasteur pipette retrofitted with a glass frit to reduce the bubble size and increase the gas-liquid contact area (interfacial area). The flow is maintained at around 5 ml/min to contain the bubbles formed within the test tube.

30   The absorption of NO is monitored in real time by logging the weight increase with a PC interfaced with the microbalance (accuracy 0.1 mg). However, to avoid balance drifting, the absorption results are supplied by measuring the total weight of the test tube with IL and pipette before and after NO absorption. Any increase in weight of the sample after NO exposure is attributed to the absorption of NO and subsequent

35   conversion to HNO_3 and variations in the water content of the sample.

27

The weight increase is in all cases given as the fractional molar increase, defined in equation [19]

$$X_{NO}^{IL} = \frac{n_{NO}}{n_{NO}+n_{IL}} \qquad [19]$$

5

A Metrohm Titrando 835 Karl Fisher titration instrument was used to determine the water content on four samples with water in 1-butyl-3-methyl–imidazolium chloride (Aldrich 99%) used for the standard curve for water. The concentration was determined as the mean value of 3 titrations.

10

28

CLAIMS

1. A method for removing NO_x gasses by an absorption process and conversion of NO_x to nitric acid (HNO_3) in the presence of oxygen and water, wherein the NO_x gasses comprise NO, NO_2, N_2O_3 and N_2O_5, the method comprising:

   a) pre-oxidation of nitric oxide (NO) to nitrogen dioxide (NO_2) and other $H_xN_yO_z$ species by use of a ionic composition catalyst at an oxidation temperature below the decomposition temperature of the ionic composition catalyst, thereby forming a pre-oxidized gas mixture, where x, y and z are integers in the ranges x= 0-1, y=1-2, z=1-5, and

   b) absorption of NO_2 and other $H_xN_yO_z$ species generated in the pre-oxidation process of step a) and conversion of the absorbed NO_2 and other $H_xN_yO_z$ species to form nitric acid (HNO_3) wherein the absorption and conversion occurs in a medium in the presence of oxygen and water at an absorption/conversion temperature which is lower than the pre-oxidation temperature in step a) which accumulates in the medium,

   wherein the ionic composition catalyst comprises one or more ionic compounds.

2. A method according to claim 1, wherein the medium is an ionic composition absorber comprising one or more ionic compounds.

3. A method according to claim 2, wherein the ionic composition absorber is
   − different from the ionic composition catalyst, or
   − identical to the ionic composition catalyst.

4. A method according to any preceding claim, wherein the ionic composition catalyst is adjusted in volume and/or flow rate to obtain a high conversion of NO to NO_2 and other $H_xN_yO_z$ species in the pre-oxidized gas mixture before performing step b), the conversion of NO to NO_2 and other $H_xN_yO_z$ species being more than 50%, preferably more than 60%, more preferably more than 70%, even more preferably more than 80%, yet more preferably more than 90% or most preferably a full conversion.

5. A method according to any preceding claim, wherein the pre-oxidation temperature in step a) is between 70 and 200°C, between 75 and 150°C, or between 80 and 120°C.

6. A method according to any preceding claim, wherein the absorption/conversion temperature in step b) is between 20 and 120°C, between 25 and 100°C, or between 30 and 80°C.

7. A method according to any preceding claim, wherein the one or more ionic compounds in the ionic composition catalyst and/or the ionic composition absorber comprising one or more organic cations selected from:
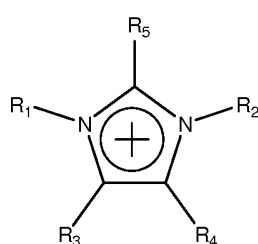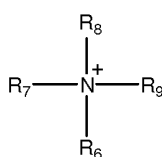
Imidazolium ion   Ammonium ion   Guanidinium ion
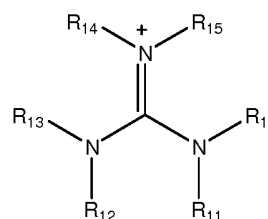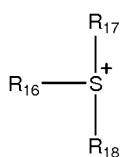
Sulfonium ion   Phosphonium ion

wherein

- R1, R2, R3, R4, R5, R6, R7, R8, R9, R10, R11, R12, R13, R14, R15, R16, R17, R18, R19, R20, R21 and R22 can be, independently, hydrogen, alkyl, halogenated alkyl, aminoalkyl, hydroxyalkyl, alkoxyalkyl, alkenyl, alkynyl, aryl, heteroaryl, cycloalkyl, cycloalkenyl, heterocycloalkyl, or heterocycloalkenyl;

- the positively charged P, N and S atoms may individually be part of heterocyclic or heteroaromatic structures by letting:

    - two of R20, R21, R22, R23, e.g. R21 and R22 be fused such that a cyclic phosphonium ion is formed; or

    - two of R6, R7, R8, R9 eg. R6 and R7 be fused, such that a cyclic ammonium ion is formed, such as a pyridinium ion; or

    - two of R11 and R12, R13 and R14, R15 and R10, eg. R11 and R12 be fused, such that a cyclic guanidinium ion is formed; or

    - two of R16, R17 and R18 eg. R16 and R17 be fused, such that a cyclic sulfonium ion is formed;

- optionally one or more cations selected from inorganic cations such as Li^+, Na^+ and K^+, and

- one or more anions selected from C_1-C_6 alkanoates such as acetate, arylcarboxylates such as benzoate, C_1-C_6 alkylsulfates such as ethyl sulfate, C_1-C_6 alkylsulfonates, C_1-C_6 perfluoroalkylsulfonates such as triflate, C_1-C_6 perfluoroalkanoates such as trifluoroacetate, C_1-C_6 perfluoroalkylsulfonimides such as bis(trifluoromethylsulfonyl) imide (triflic imide), tetrafluoroborate, hexafluorophosphate, sulfate, nitrate and halides such as chloride or bromide.

8. A method according to any preceding claim wherein the one or more ionic compounds in the ionic composition catalyst and/or the ionic composition absorber comprising a cation having the following structure:
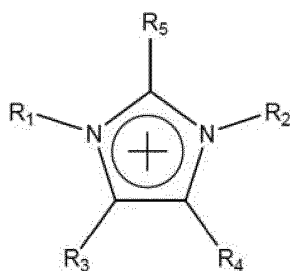
   wherein R_1 and R_2 are individually selected from C_1-C_8 alkyl groups or aryl groups, and wherein R_3, R_4 and R_5 are individually selected from hydrogens, C_1-C_6 alkyl groups or aryl groups or wherein R_3 and R_4 together with the imidazolium group may form a 4- to 6-membered saturated, unsaturated or aromatic ring, which may further contain up to three hetero atoms selected from oxygen, nitrogen and phosphorus.

9. A method according to any preceding claim, wherein the one or more ionic compounds in the ionic composition catalyst and/or the ionic composition absorber is selected from 1-ethyl-3-methylimidazolium ($[EMIM]^+$) acetate, 1-butyl-3-methyl-imidazolium ($[BMIM]^+$) acetate, 1-ethyl-3-methylimidazolium ($[EMIM]^+$) triflate, 1-butyl-3-methylimidazolium ($[BMIM]^+$) triflate, 1-ethyl-3-methylimidazolium ($[EMIM]^+$) nitrate, 1-butyl-3-methylimidazolium ($[BMIM]^+$) nitrate, 1-butyl-2,3-dimethyl-imidazolium ($[BMMIM]^+$) nitrate, choline chloride, choline acetate and 1,1,3,3-tetramethylguanidinium chloride.

10. A method according to any preceding claim, wherein the ionic composition catalyst and/or the ionic composition absorber further comprises one or more cations selected from Li^+, Na^+ and K^+.

5   11. A method according to any preceding claim, wherein the one or more ionic compounds in the ionic composition catalyst and/or the ionic composition absorber is an ionic liquid.

12. A method according to any preceding claim, wherein the ionic composition catalyst
10   and/or the ionic composition absorber:
        – is dispersed on a porous carrier and used in the form of a supported ionic composition phase material, or
        – is an ionic liquid dispersed on a porous carrier and used in the form of a supported ionic liquid phase (SILP) material.
15

13. A method according to claim 12, wherein the porous carrier material is composed of carbon, zeolites, clays, hydroxides or oxides based on the elements Si, Al, Ti, Ce, Zr, Mg, Fe, Ca, Sr, Ba, Mn, Ge and/or Ga.

20   14. A method according to any one of the preceding claims wherein a wet scrubbing system for removal of SO_2 and SO_3 comprised in the off-gasses is implemented before performing step a).

15. A method according to any preceding claim, wherein the off-gasses are flue gases
25   originating either from large stationary sources like power or incineration plants or cement production plants, or from mobile emission sources like e.g. commercial marine vessels, mobile incineration plants for incineration of e.g. domestic or industrial waste, or diesel trans and/or trucks.
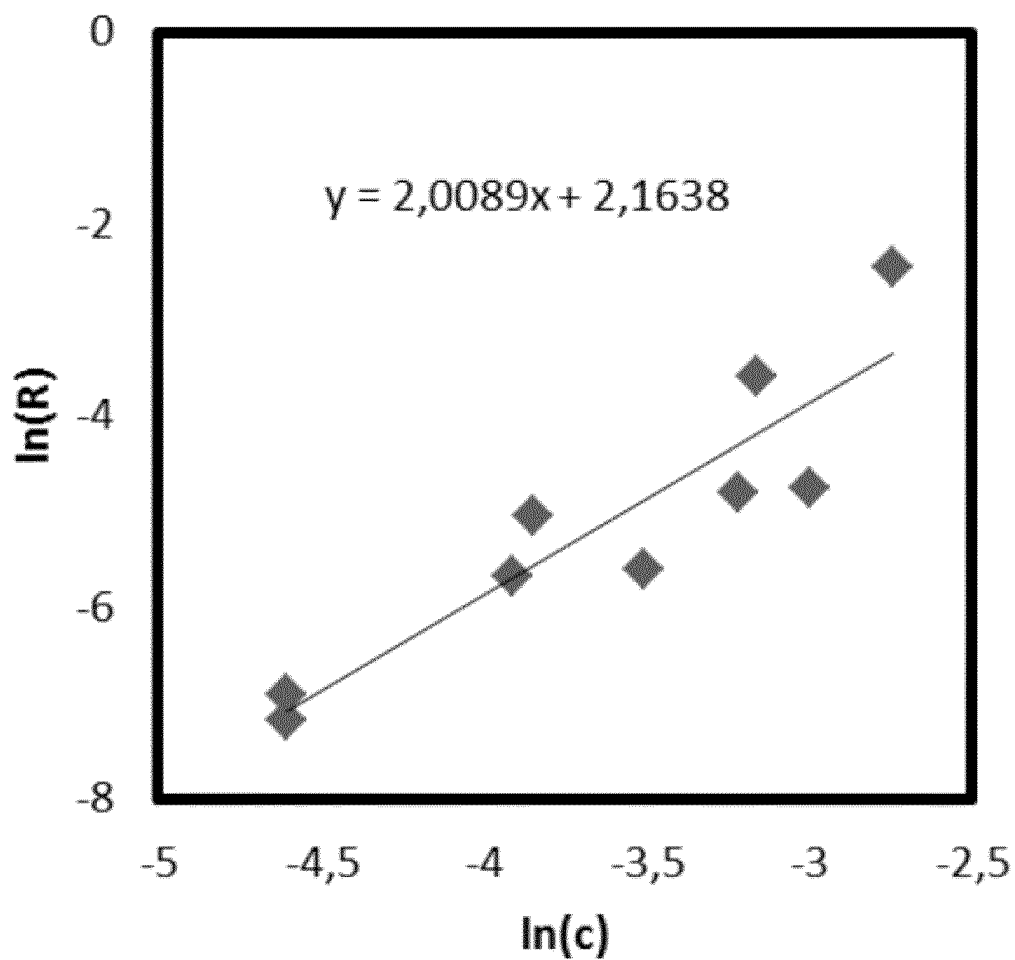
Fig. 1
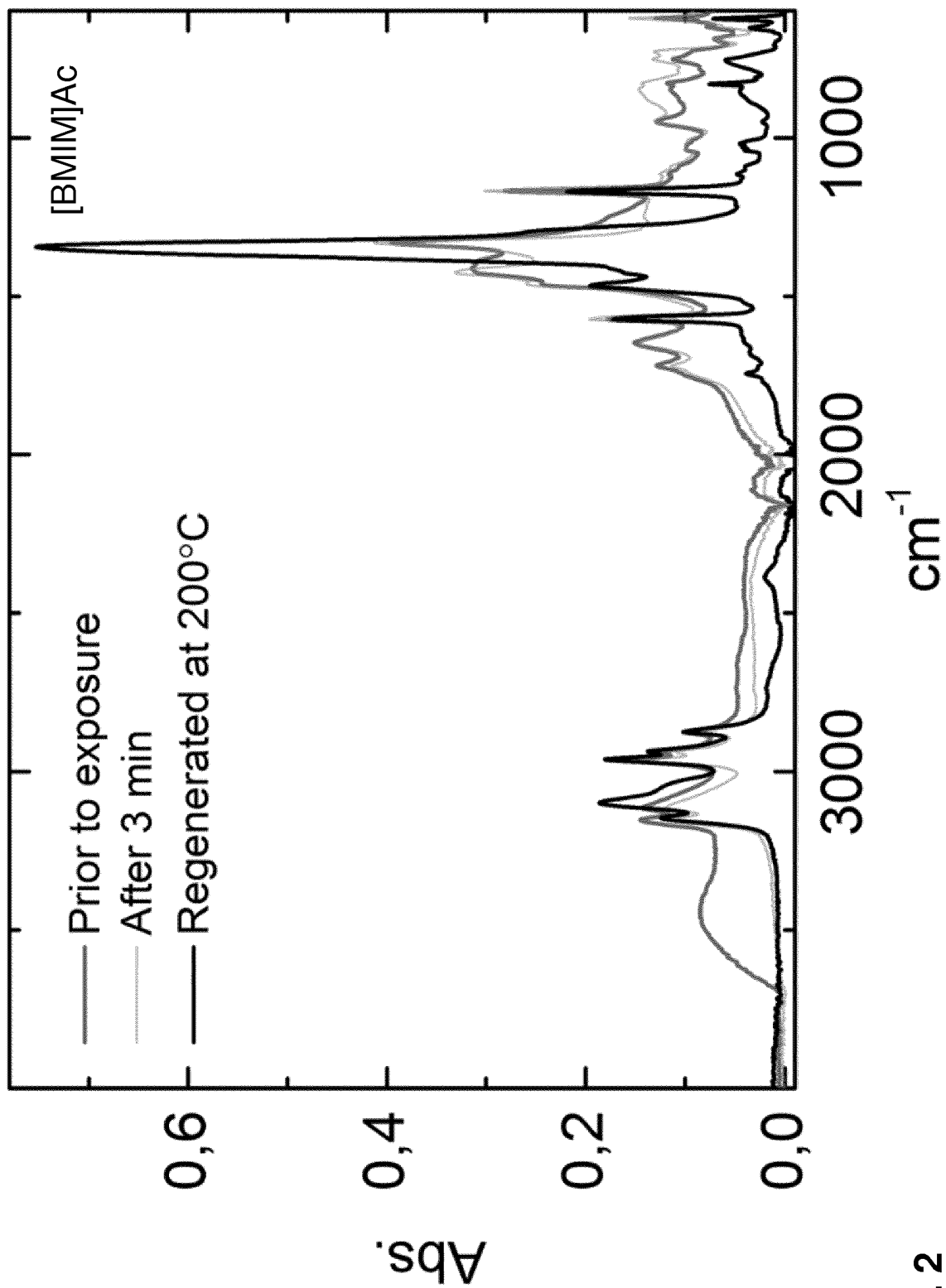
Fig. 2
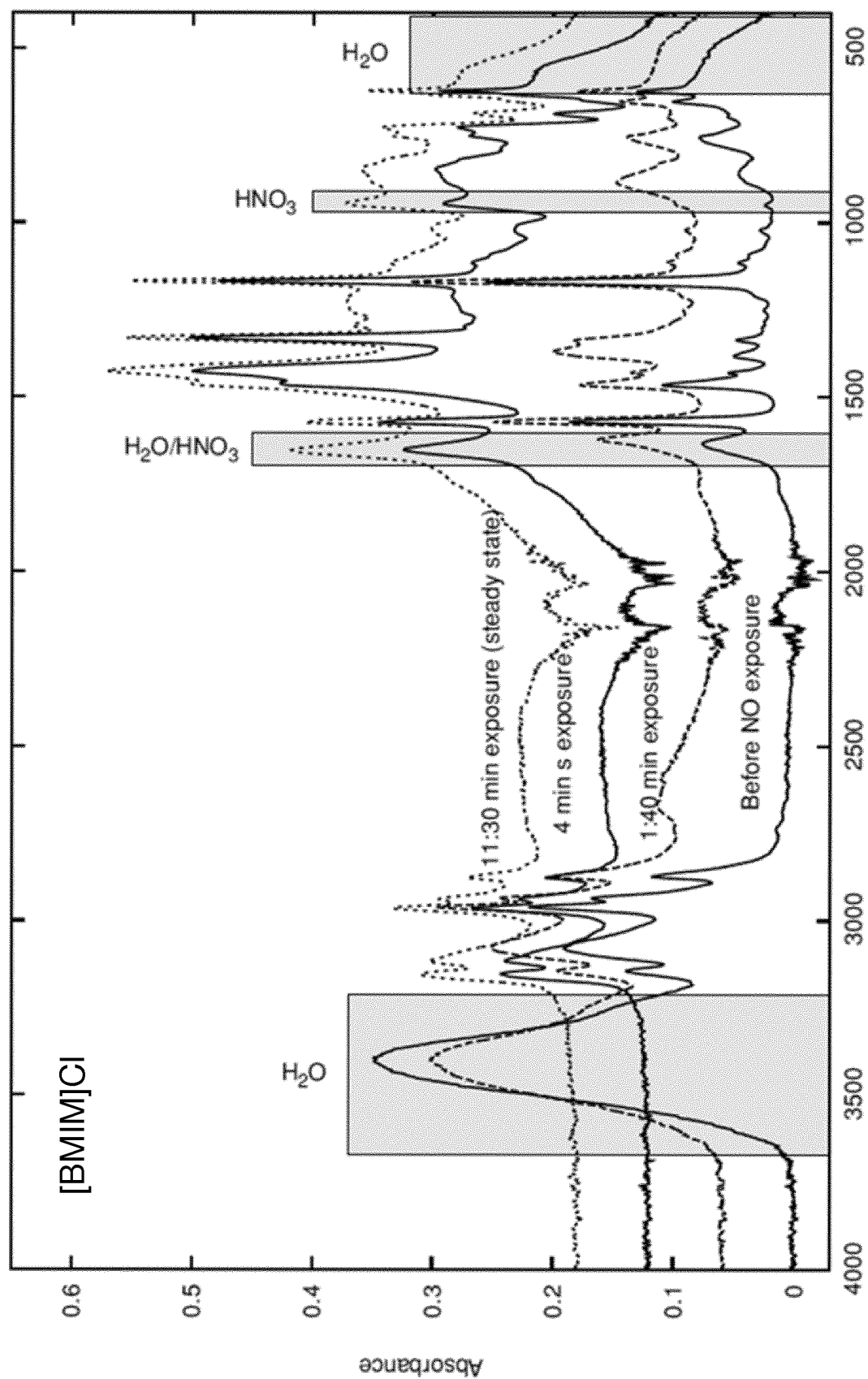
Fig. 3
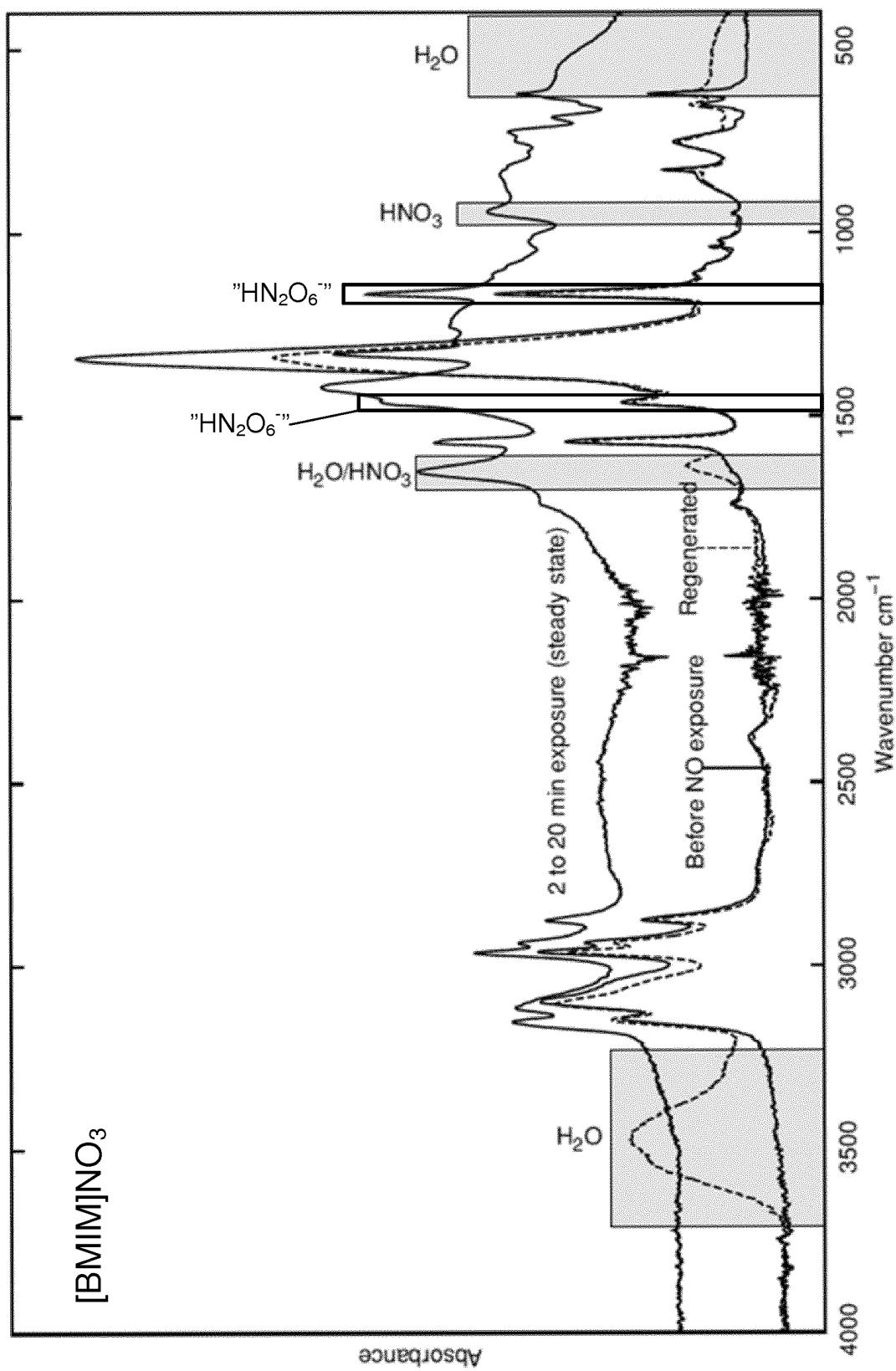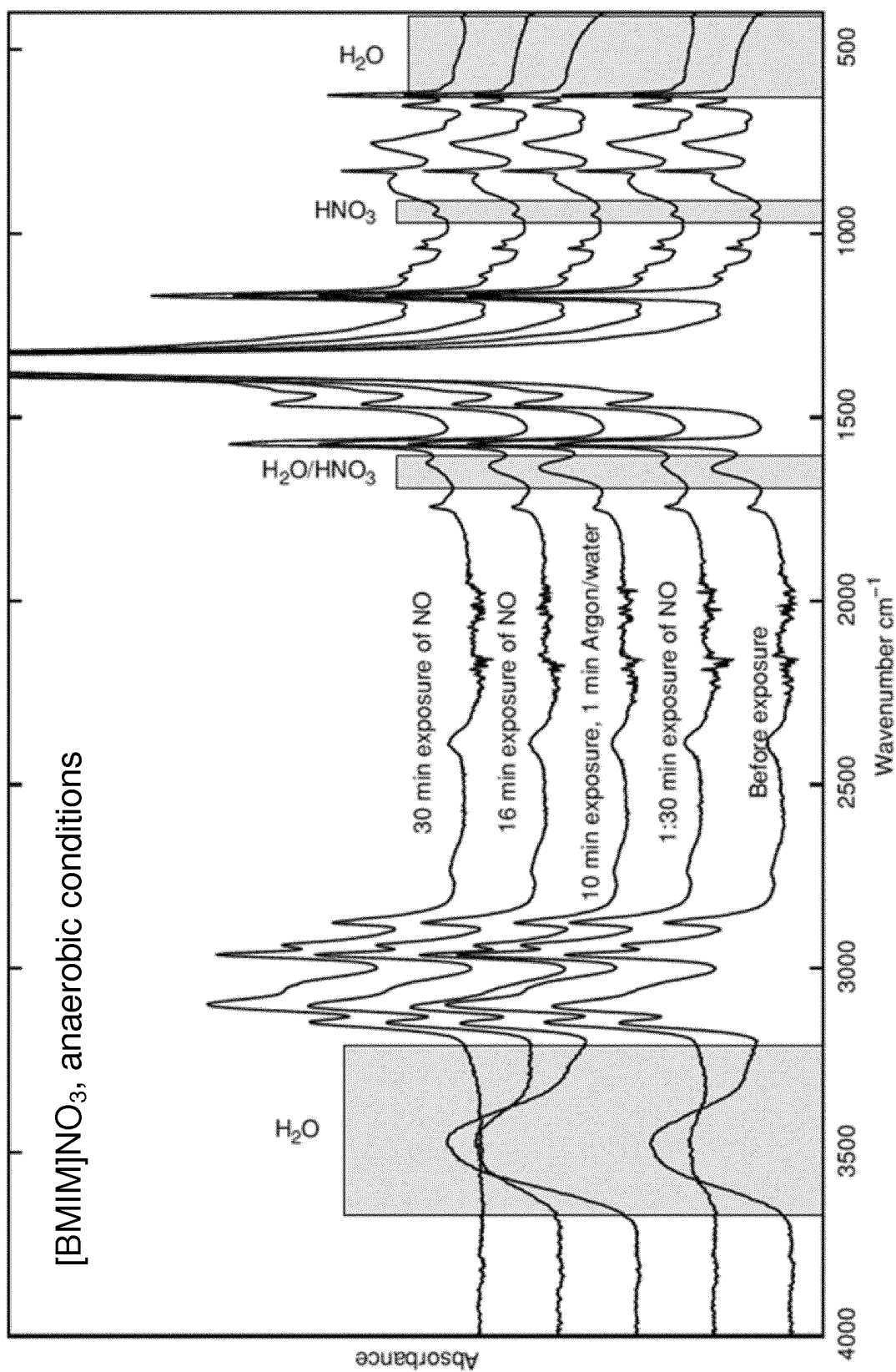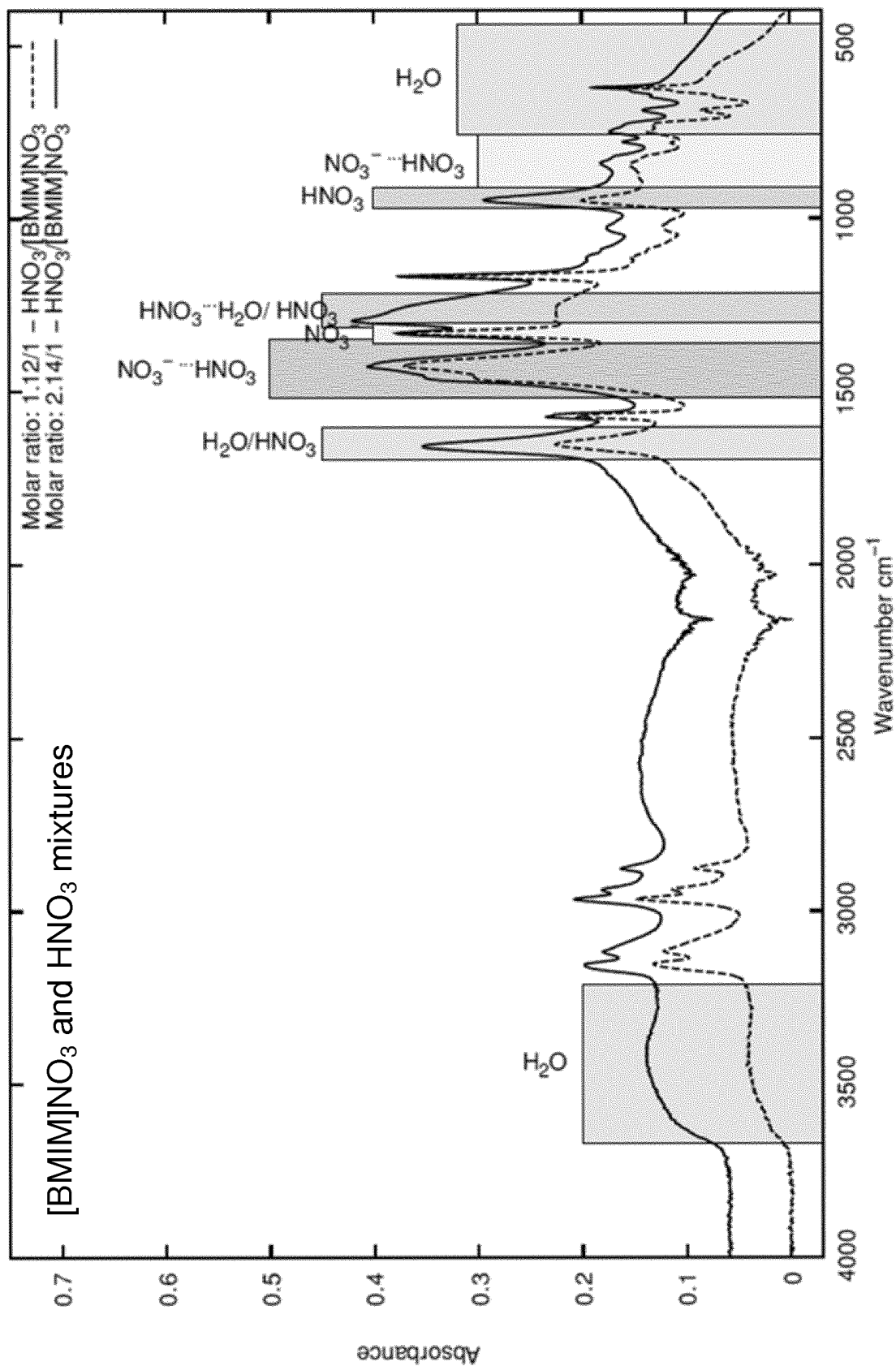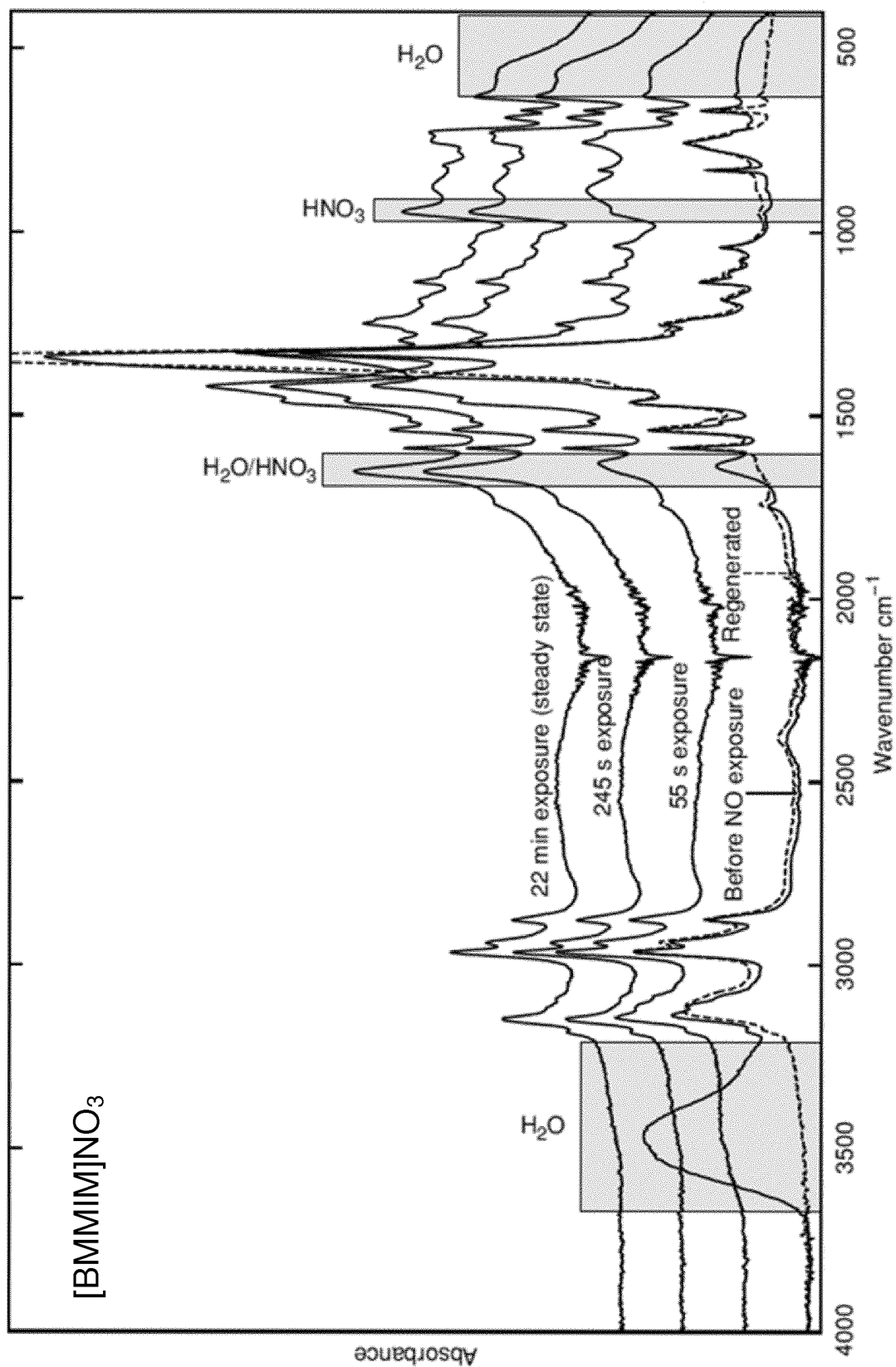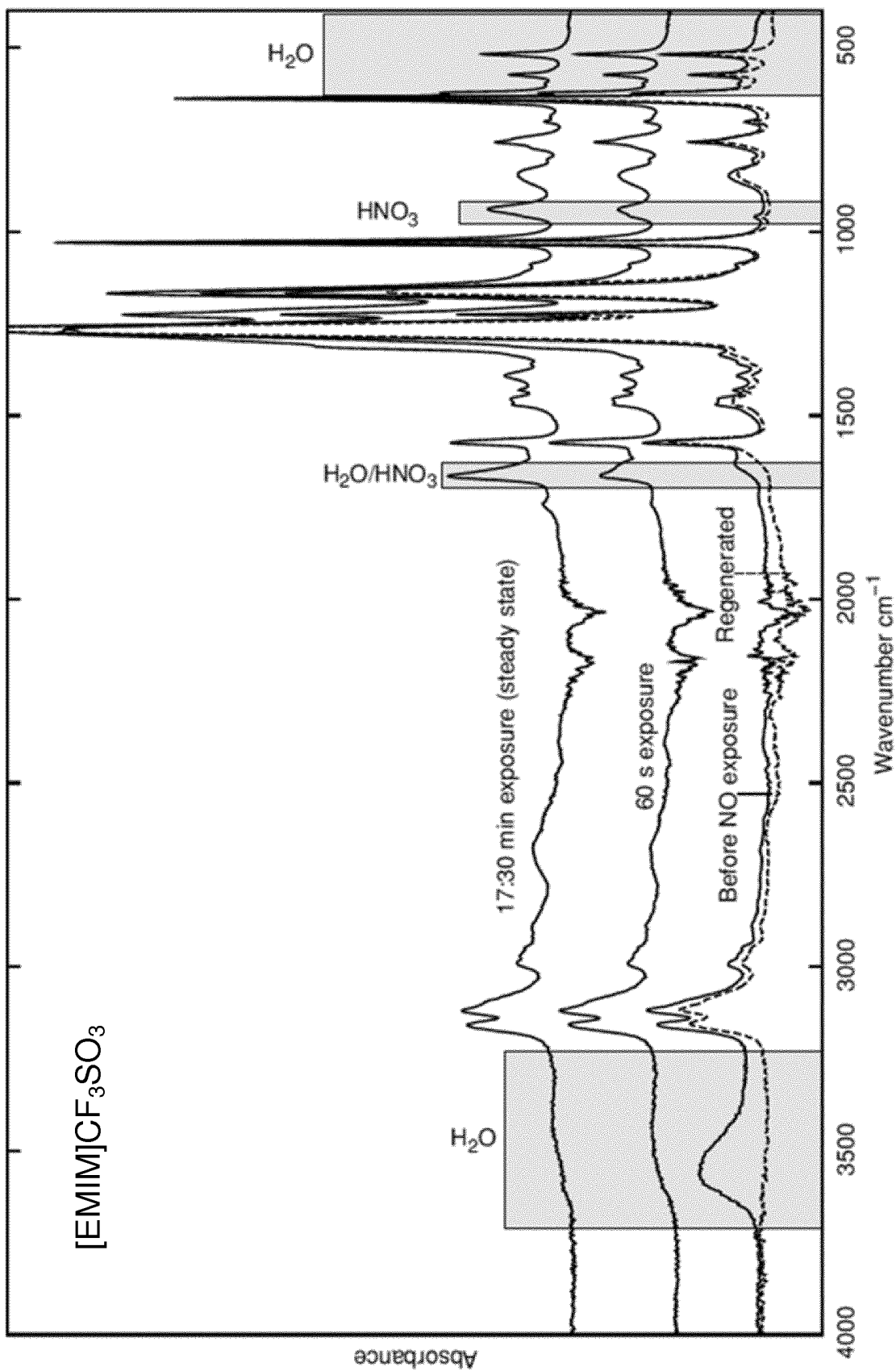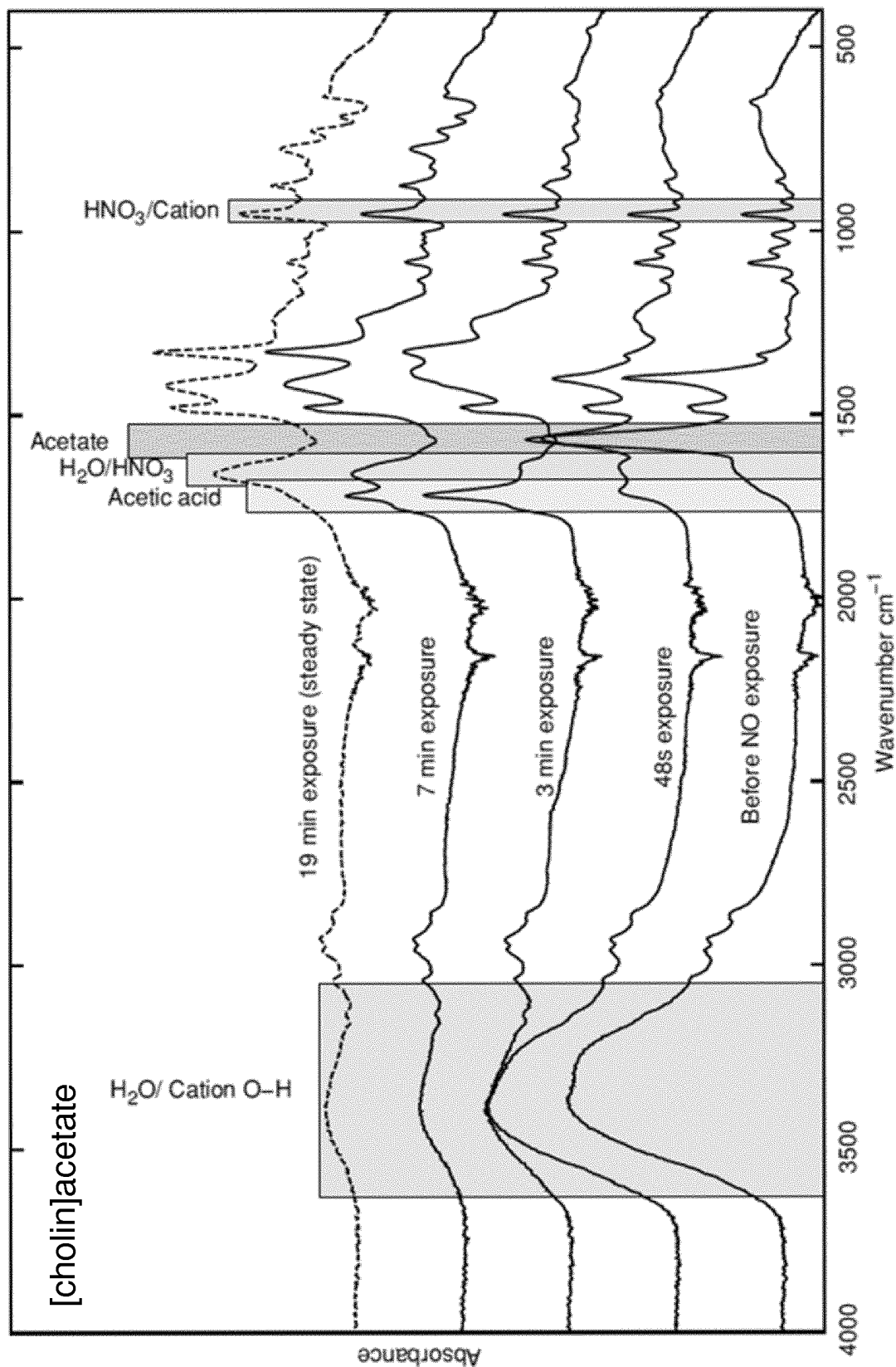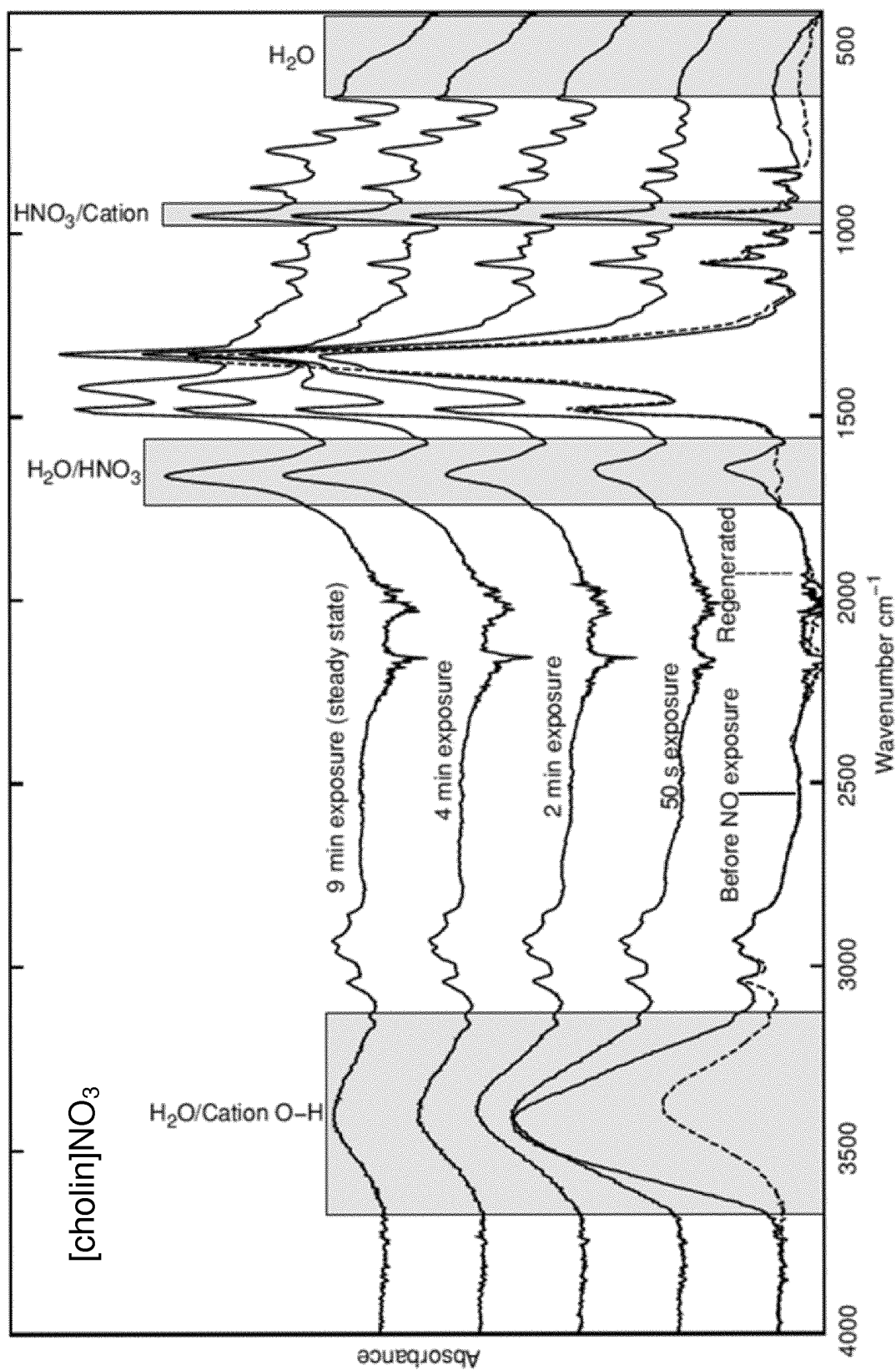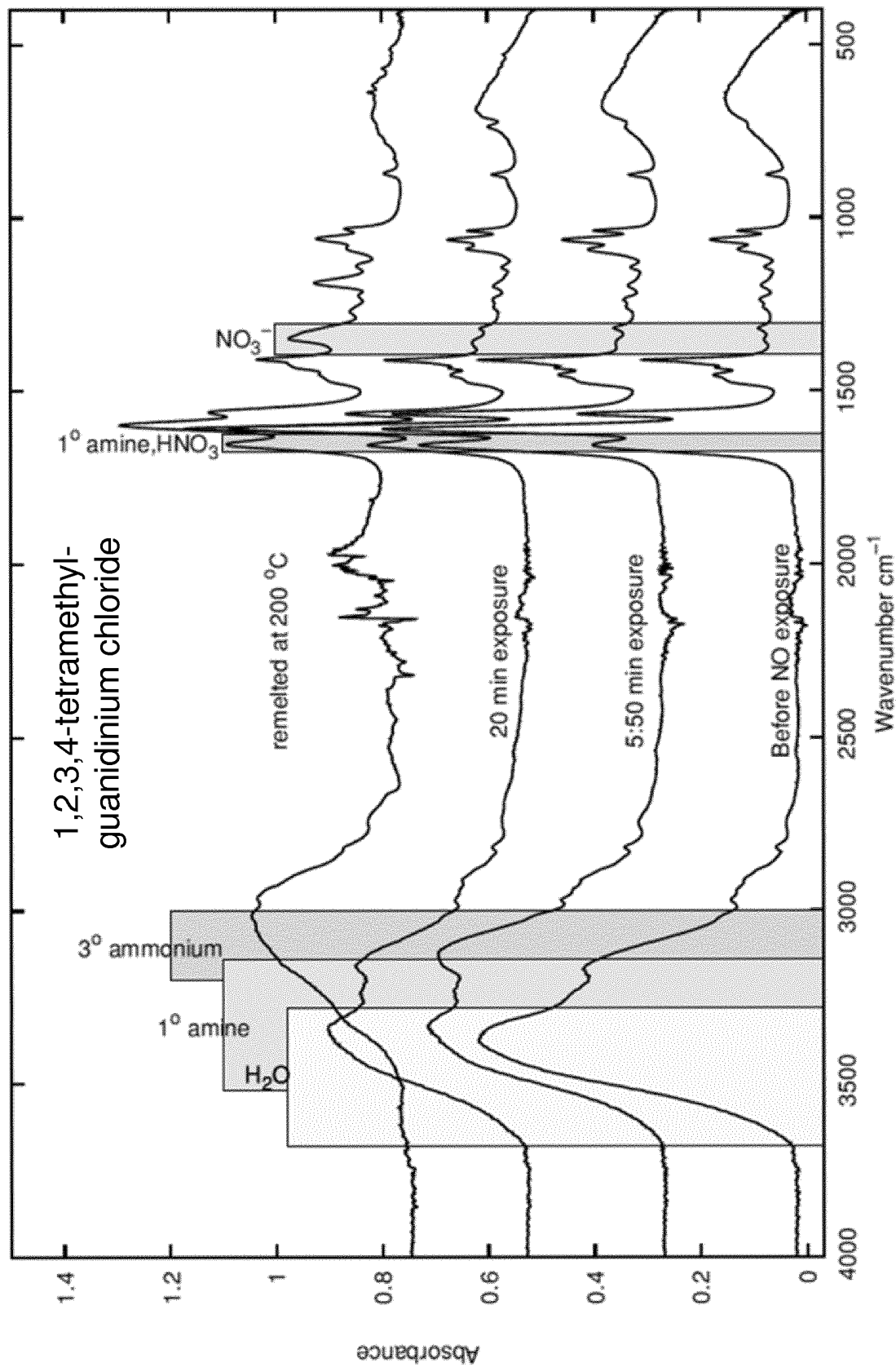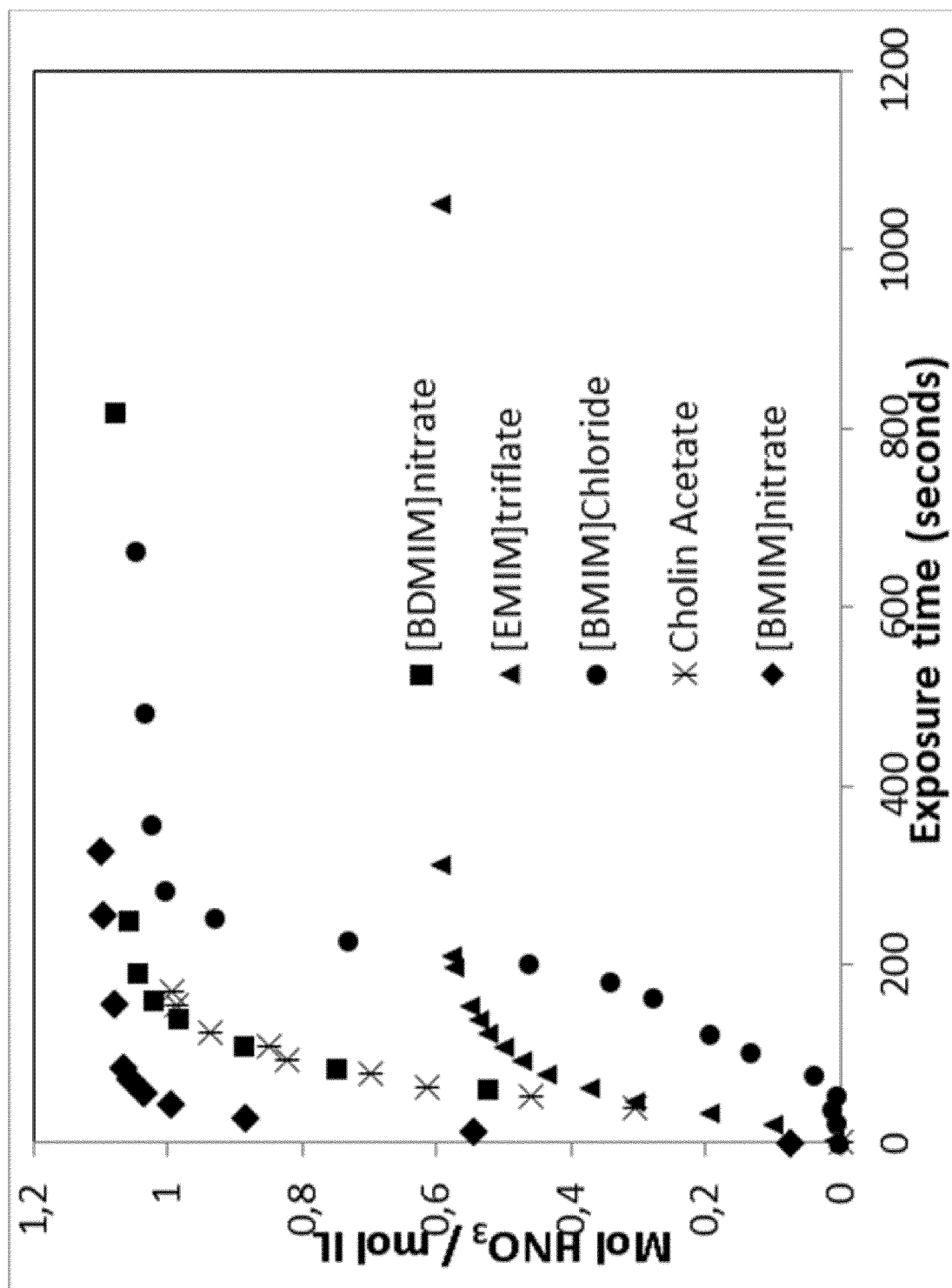
Fig. 4a

Fig. 4b

Fig. 4c

Fig. 5

Fig. 6

Fig. 7

Fig. 8

Fig. 9

Fig. 10

Fig. 11

Fig. 12

Fig. 13

BMIM CH₃COO after NO absorption and heating

BMIM NO₃ (Fluka)

Chemical shift

Fig. 14

Nitrate anion bands

$1420\ cm^{-1}$ and $1310\ cm^{-1}$

$1340\ cm^{-1}$

Nitric acid bands

HNO_3: $1660\ cm^{-1}$, DNO_3: $1610\ cm^{-1}$

HNO_3, DNO_3: $940\ cm^{-1}$
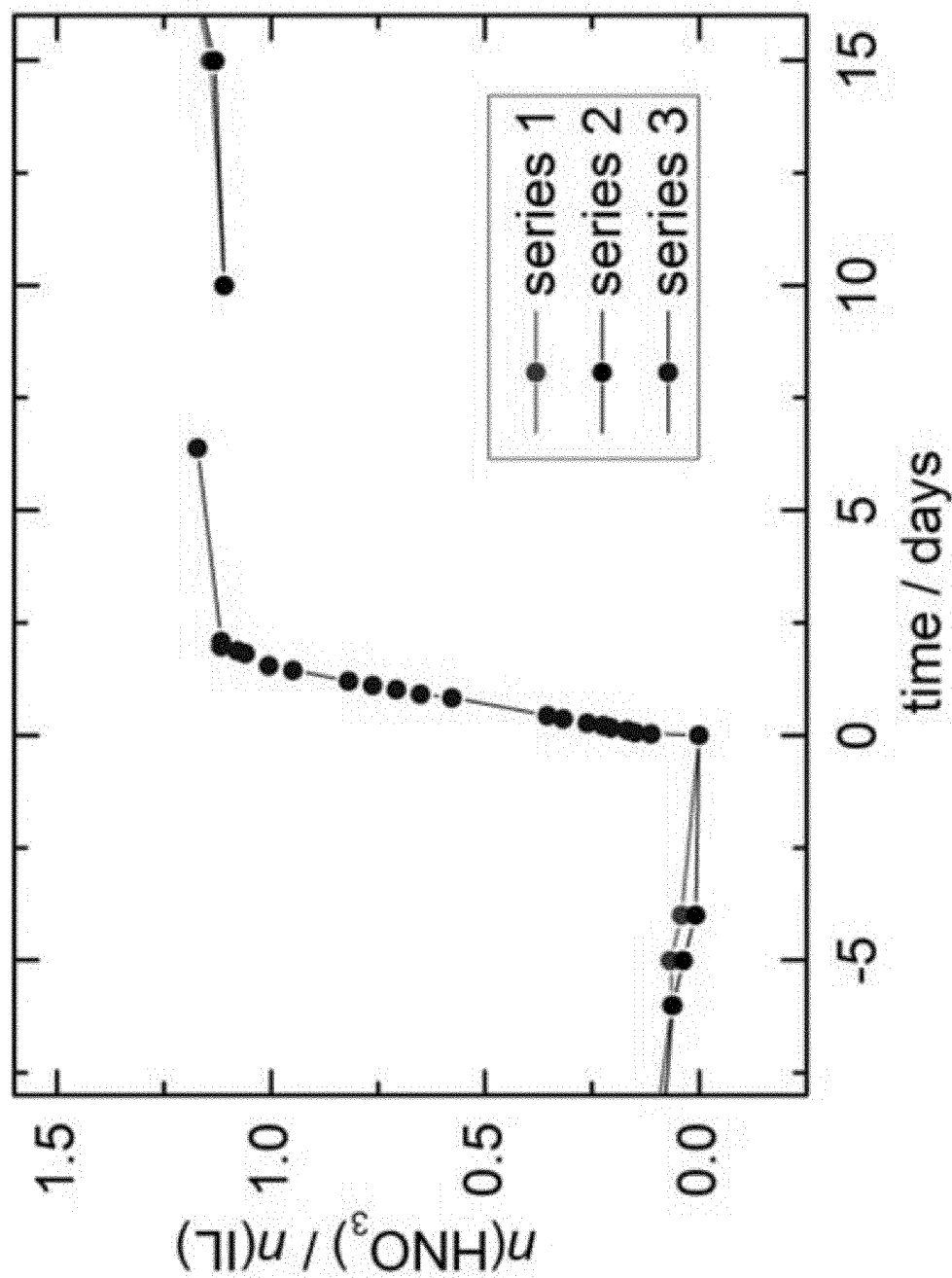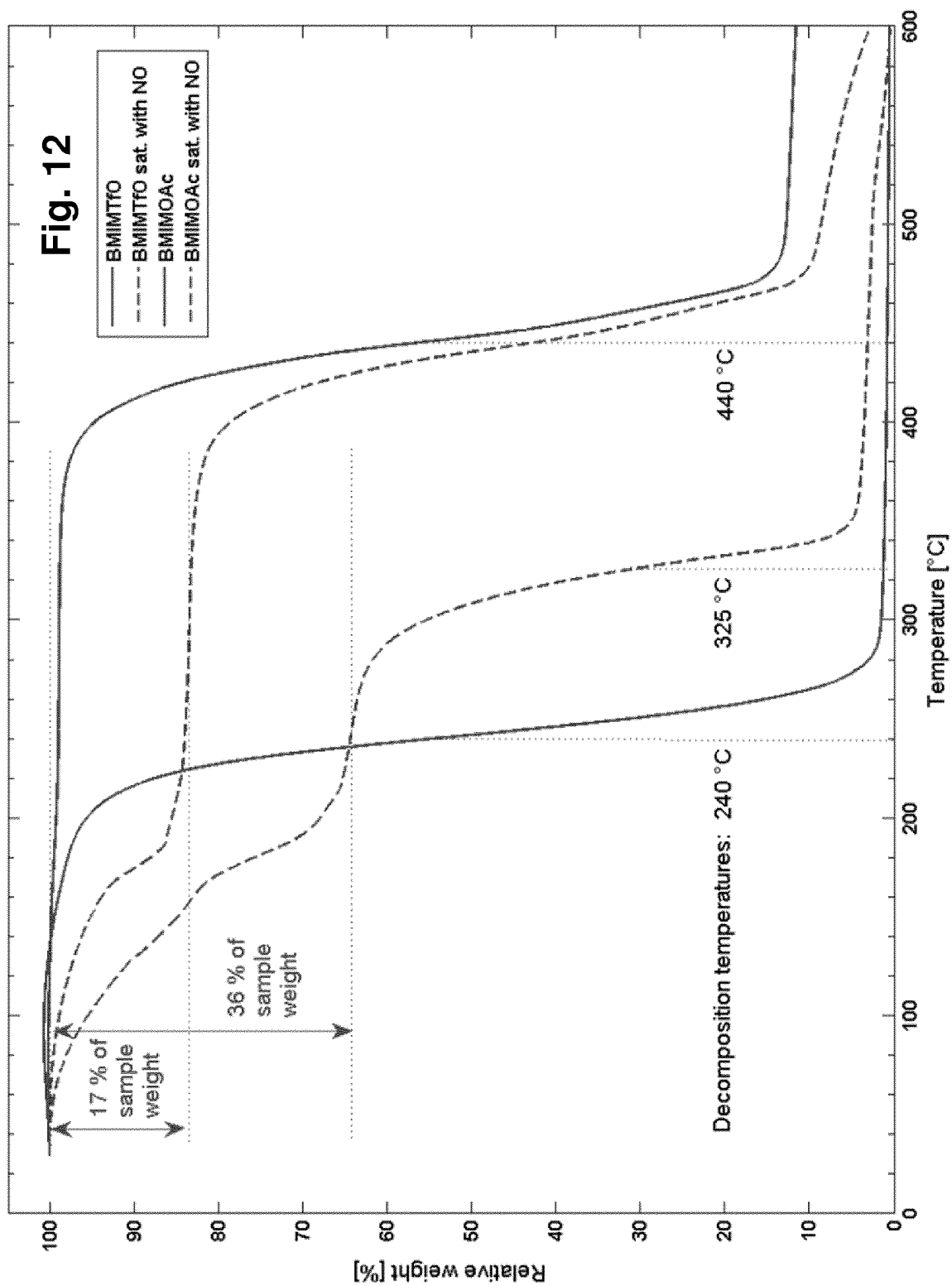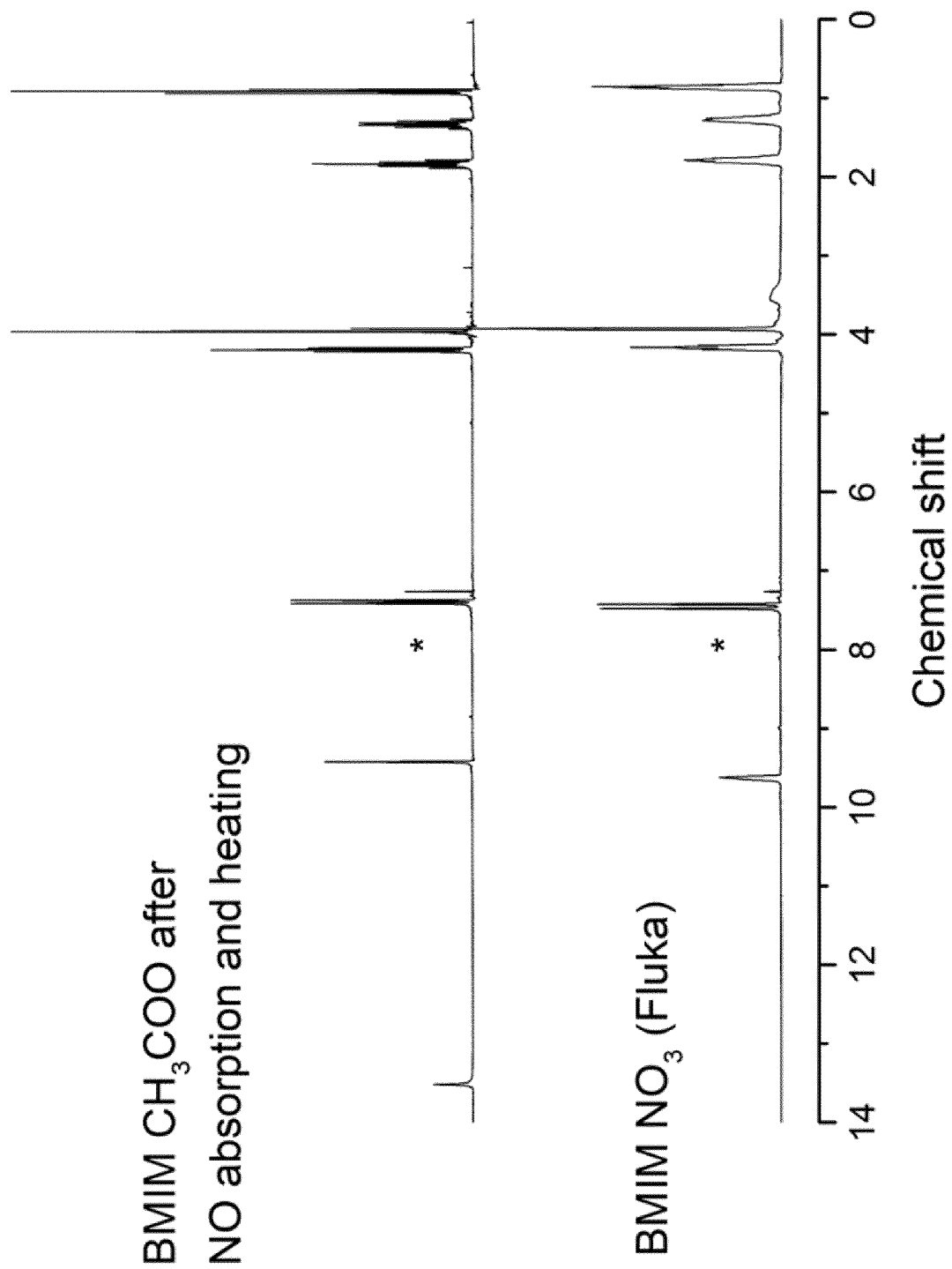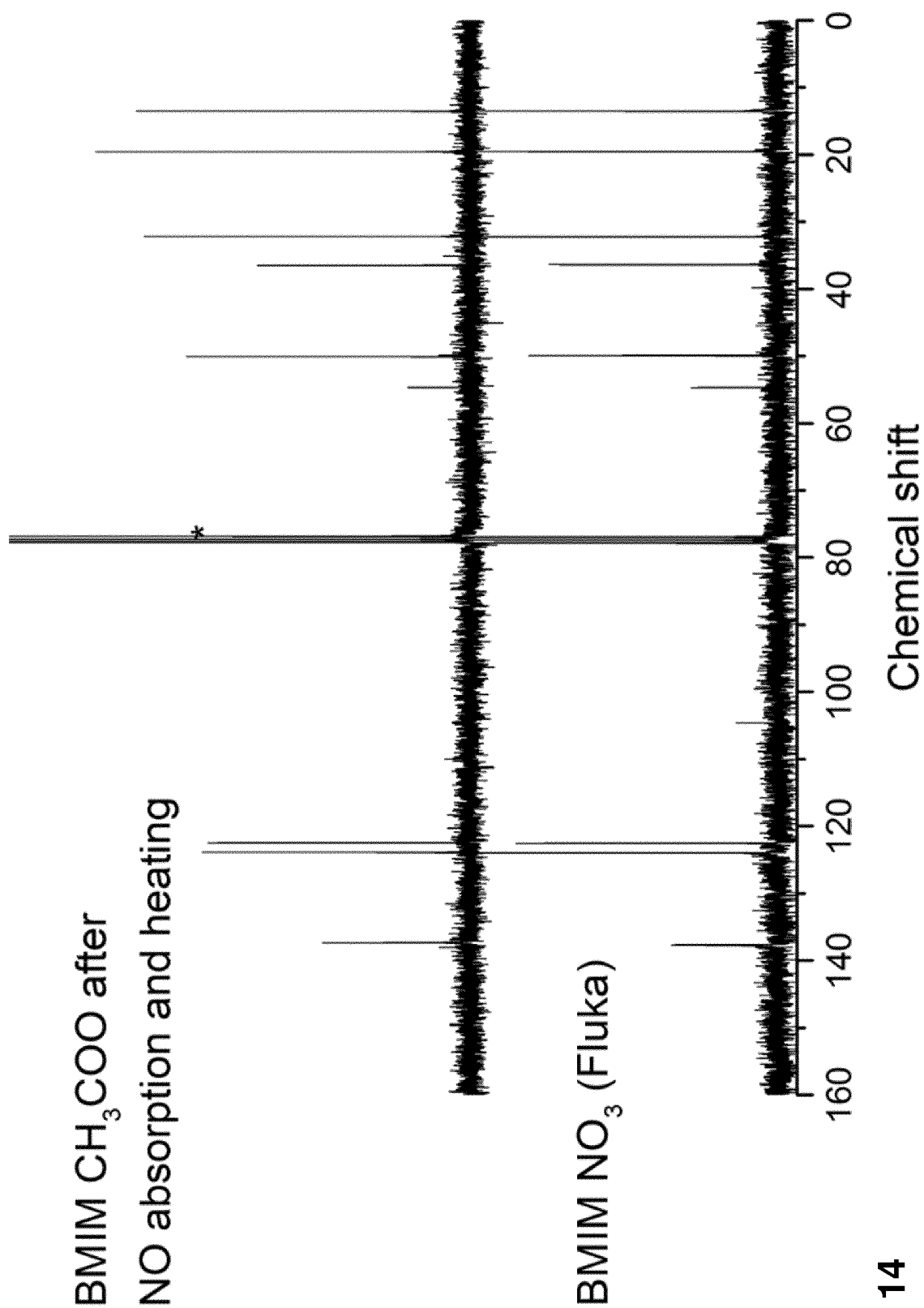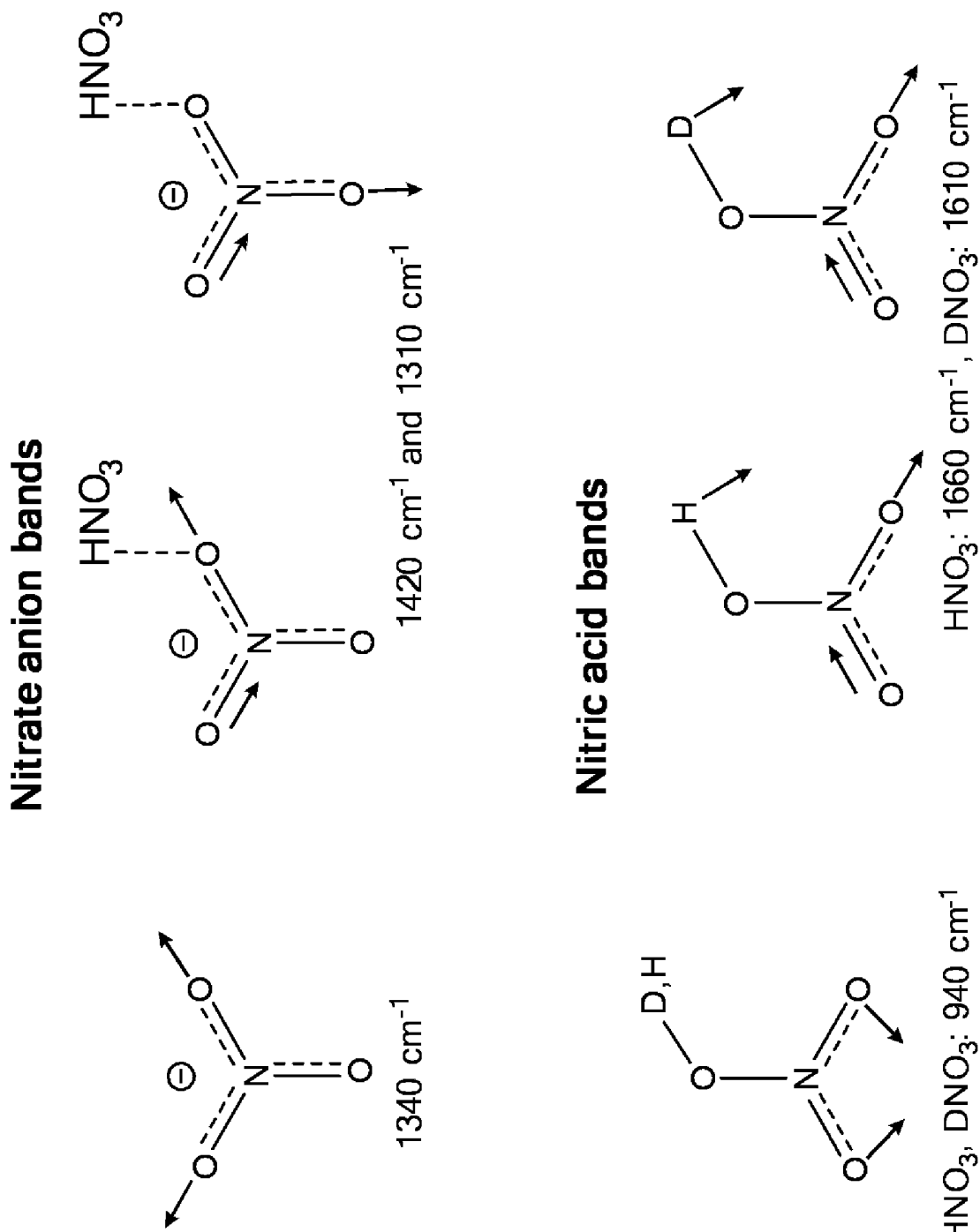
Fig. 15
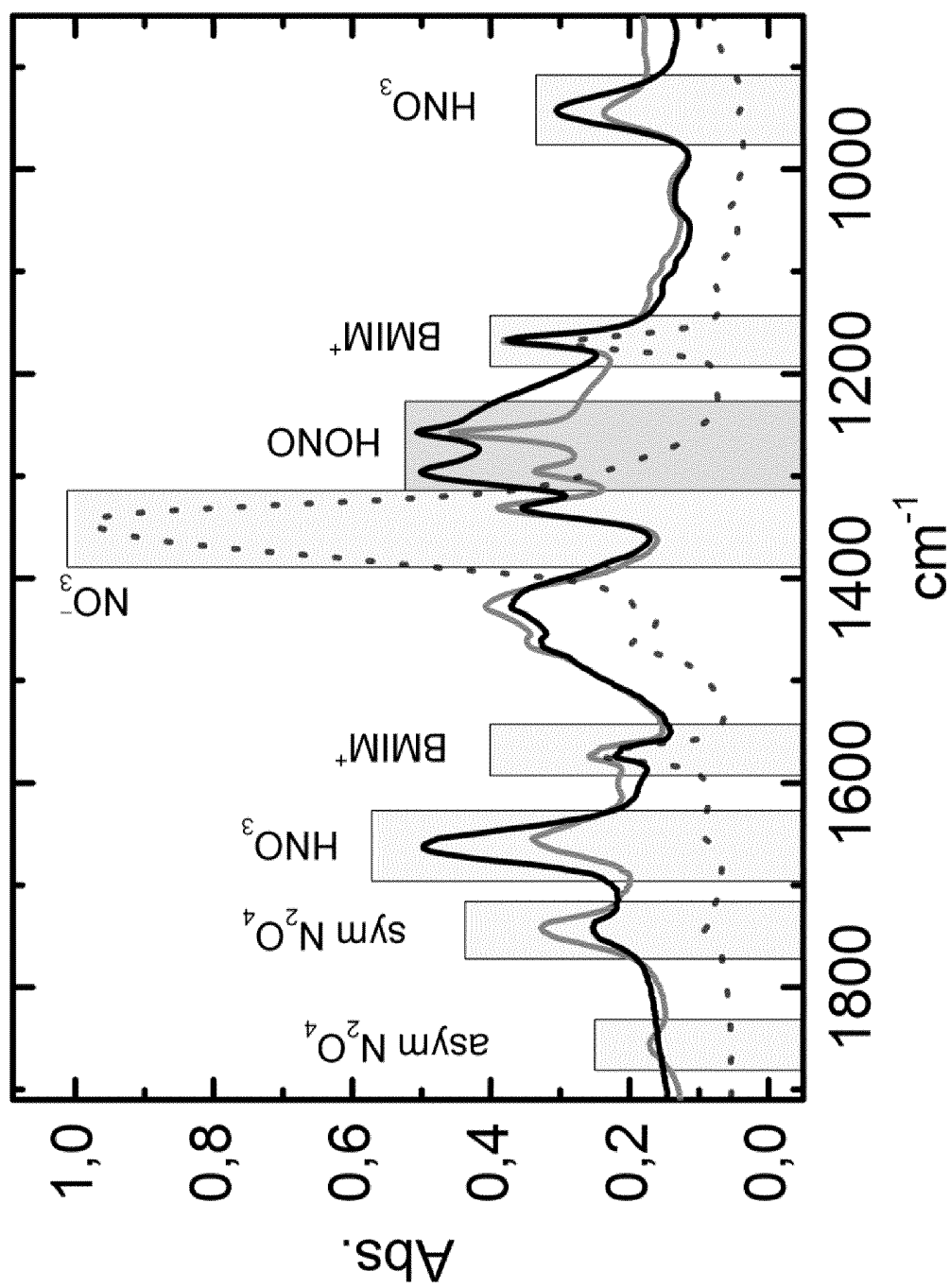
Fig. 16
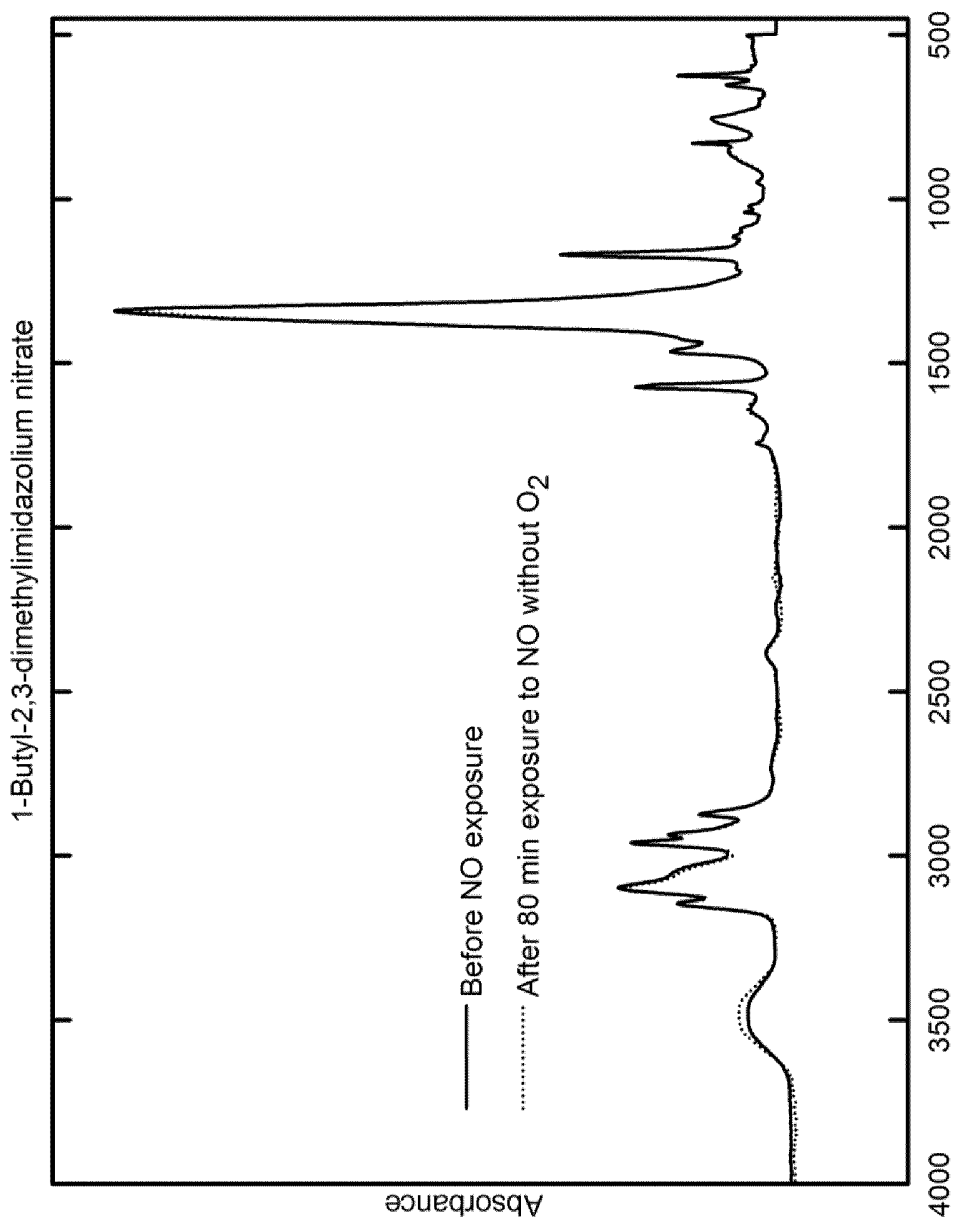
Fig. 17
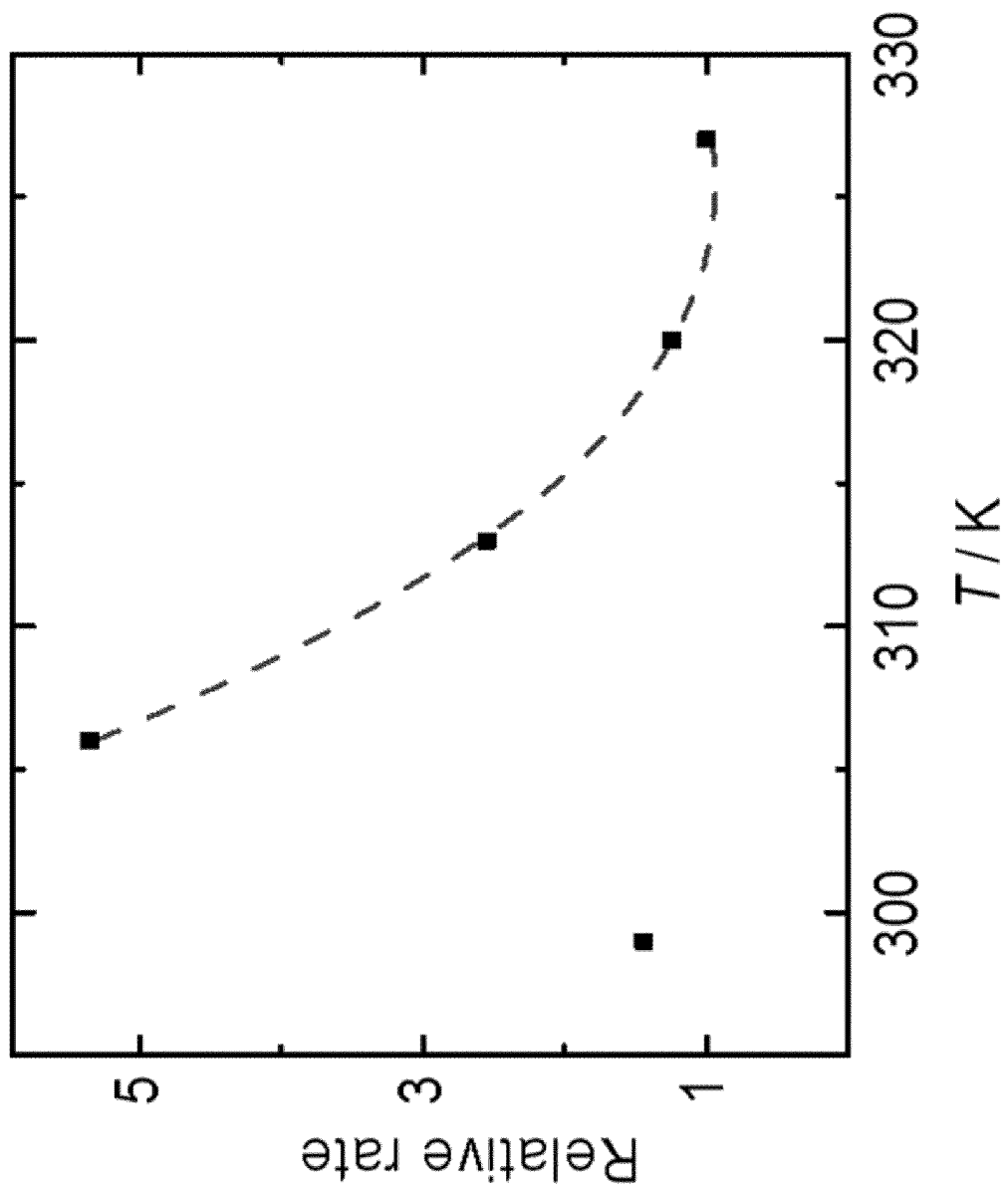
Fig. 18
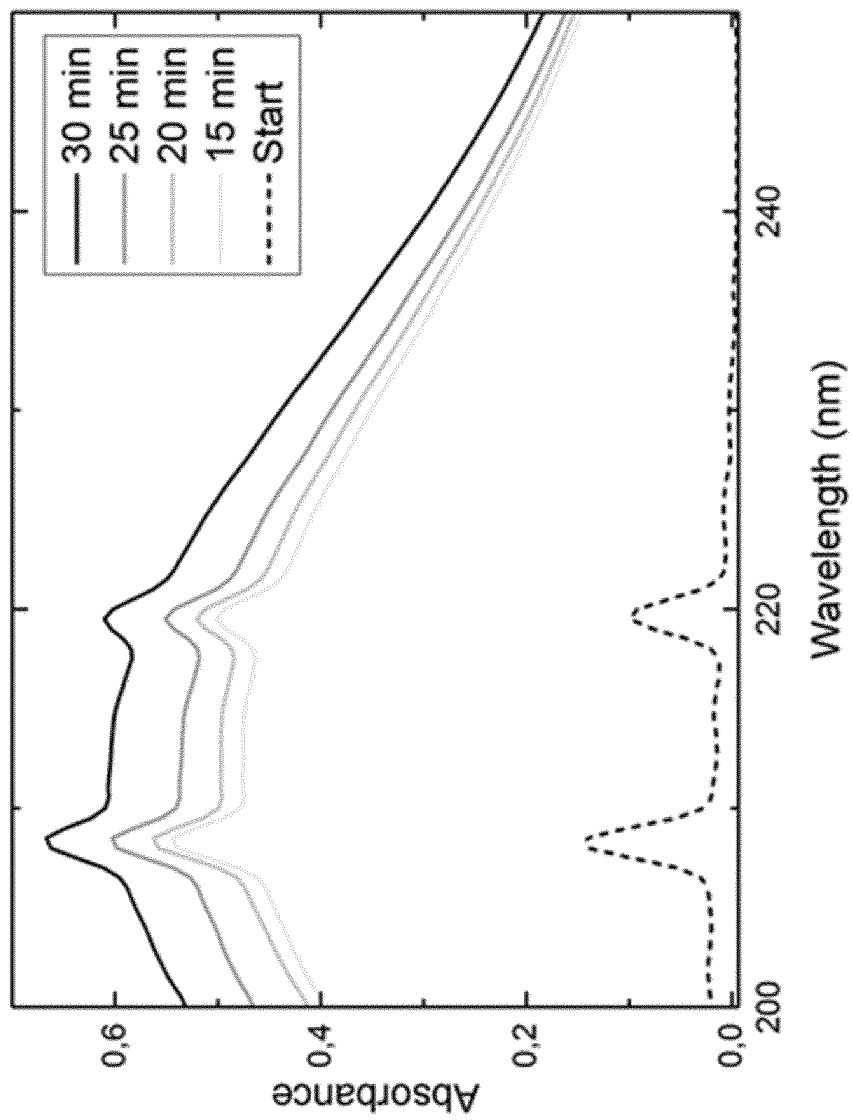
Fig. 19
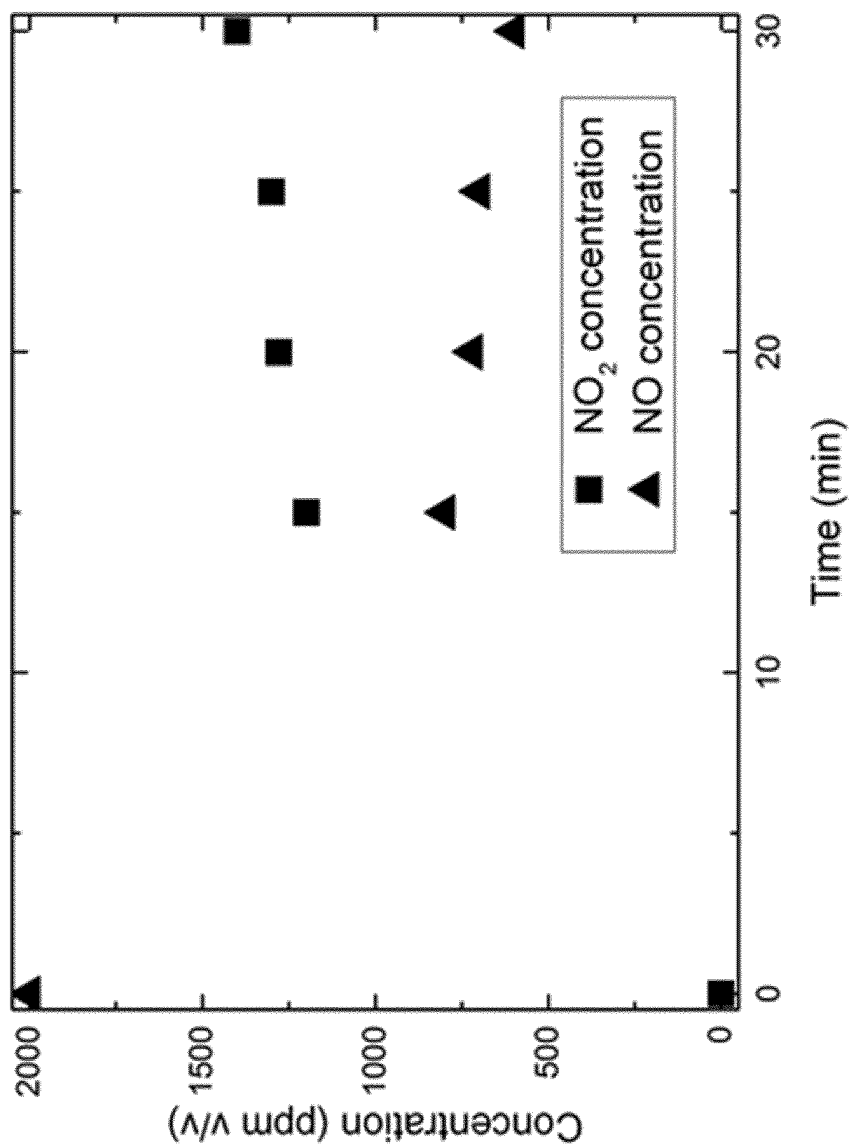
Fig. 20
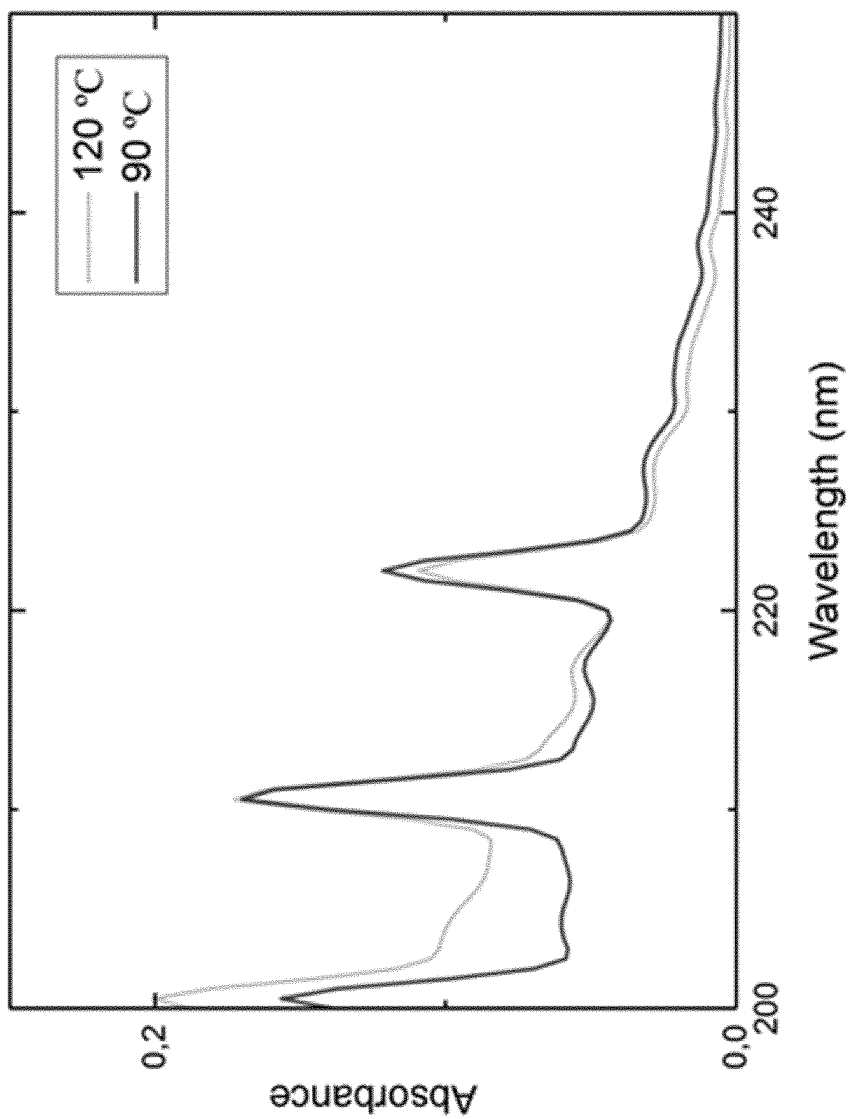
Fig. 21

INTERNATIONAL SEARCH REPORT

A. CLASSIFICATION OF SUBJECT MATTER
INV. B01D53/04
ADD.

According to International Patent Classification (IPC) or to both national classification and IPC

B. FIELDS SEARCHED

Minimum documentation searched (classification system followed by classification symbols)
B01D

Documentation searched other than minimum documentation to the extent that such documents are included in the fields searched

Electronic data base consulted during the international search (name of data base and, where practicable, search terms used)

EPO-Internal, WPI Data

C. DOCUMENTS CONSIDERED TO BE RELEVANT

Category*	Citation of document, with indication, where appropriate, of the relevant passages	Relevant to claim No.
X	WO 2013/079597 A1 (UNIV DANMARKS TEKNISKE [DK]) 6 June 2013 (2013-06-06) the whole document -----	1-15
X	WO 2007/101397 A1 (BOC GROUP INC [US]; LU YAPING [US]; ZHAI SULING [CN]; WANG QINGMIN [US) 13 September 2007 (2007-09-13) cited in the application the whole document ----- -/--	1-15

| X | Further documents are listed in the continuation of Box C. | | X | See patent family annex. |

* Special categories of cited documents :

"A" document defining the general state of the art which is not considered to be of particular relevance

"E" earlier application or patent but published on or after the international filing date

"L" document which may throw doubts on priority claim(s) or which is cited to establish the publication date of another citation or other special reason (as specified)

"O" document referring to an oral disclosure, use, exhibition or other means

"P" document published prior to the international filing date but later than the priority date claimed

"T" later document published after the international filing date or priority date and not in conflict with the application but cited to understand the principle or theory underlying the invention

"X" document of particular relevance; the claimed invention cannot be considered novel or cannot be considered to involve an inventive step when the document is taken alone

"Y" document of particular relevance; the claimed invention cannot be considered to involve an inventive step when the document is combined with one or more other such documents, such combination being obvious to a person skilled in the art

"&" document member of the same patent family

Date of the actual completion of the international search	Date of mailing of the international search report
11 June 2015	27/07/2015

Name and mailing address of the ISA/	Authorized officer
European Patent Office, P.B. 5818 Patentlaan 2 NL - 2280 HV Rijswijk Tel. (+31-70) 340-2040, Fax: (+31-70) 340-3016	Fischer, Michael

1

C(Continuation). DOCUMENTS CONSIDERED TO BE RELEVANT

Category*	Citation of document, with indication, where appropriate, of the relevant passages	Relevant to claim No.
X	Esther Kuhlmann: "Entwicklung von Extraktions- und Absorptionssystemen auf Basis ionischer Flüssigkeiten für die Entschwefelung von Kohlenwasserstoffen", , 15 February 2008 (2008-02-15), XP055145829, Retrieved from the Internet: URL:http://www.opus.ub.uni-erlangen.de/opus/volltexte/2008/930/ [retrieved on 2014-10-10] the whole document -----	1-15
X	US 2012/258030 A1 (MARUYAMA MASATOSHI [JP] ET AL) 11 October 2012 (2012-10-11) paragraphs [0068], [0069], [0076] -----	1-15
A	ERHONG DUAN ET AL: "Absorption of NO and NO 2 in Caprolactam Tetrabutyl Ammonium Halide Ionic Liquids", JOURNAL OF THE AIR & WASTE MANAGEMENT ASSOCIATION, vol. 61, no. 12, 1 December 2011 (2011-12-01), pages 1393-1397, XP055147258, ISSN: 1096-2247, DOI: 10.1080/10473289.2011.623635 abstract -----	1

1

Patent document cited in search report		Publication date	Patent family member(s)		Publication date
WO 2013079597	A1	06-06-2013	AU	2012343846 A1	12-06-2014
			CA	2856792 A1	06-06-2013
			CN	104080524 A	01-10-2014
			EP	2785436 A1	08-10-2014
			JP	2015505720 A	26-02-2015
			KR	20140112492 A	23-09-2014
			US	2015037232 A1	05-02-2015
			WO	2013079597 A1	06-06-2013
WO 2007101397	A1	13-09-2007	CN	101032677 A	12-09-2007
			WO	2007101397 A1	13-09-2007
US 2012258030	A1	11-10-2012	DE	102012102733 A1	11-10-2012
			JP	2012217918 A	12-11-2012
			US	2012258030 A1	11-10-2012